Spin dependent electronic transport (Magnetotransport properties of metals and semiconductors: introduction)

Alexander Granovsky

Lomonosov Moscow State University, Moscow 119991, Russia

1755

40 Faculties
50.000 students
10.000 staff
2 ships, 6 subdiv.
Supercomputer
Sputnik

Magnetism Department, Faculty of Physics, MSU

Magnetism Department was founded more than 70 years ago.

The hysteresis loop was measured in MSU by Prof. Stoletov in 1872.

Stoletov, Arkad'ev, Landau, Kapitza, Kondorski

The main topics:

- Advanced Magnetic Materials (nanostructures, soft and hard, amorphous and nanocrystalline, thin films, ribbons, microwires, carbon nanotubes, multilayers "ferromagnet/superconductor" etc)
- Spintronics
- Magnetophotonics (magnetooptics, magnetophotonic crystals)
- Room temperature dilute magnetic semiconductors and oxides
- Magnetic liquids and polymers
- Magnetic sensors
- Biomagnetism

36 departments,
2500 students
400 PhD students
800 staff

Outline

- Introduction
- Resistivity (Mooij correlation)
- Magnetoresistance (AMR, injection MR, organic MR)
- Anomalous Hall effect : Basic mechanisms
- Anomalous Hall effect in heterogeneous alloys
- Anomalous Hall effect in diluted magnetic semiconductors.
- Can the presence of anomalous Hall effect serve as an evidence of spin polarization of current carriers ?
- Recent experimental data on TiO2:Co
- Conclusions

"I swear to tell the truth, all the truth and nothing but the truth"

Present and Future of Hard-Disks

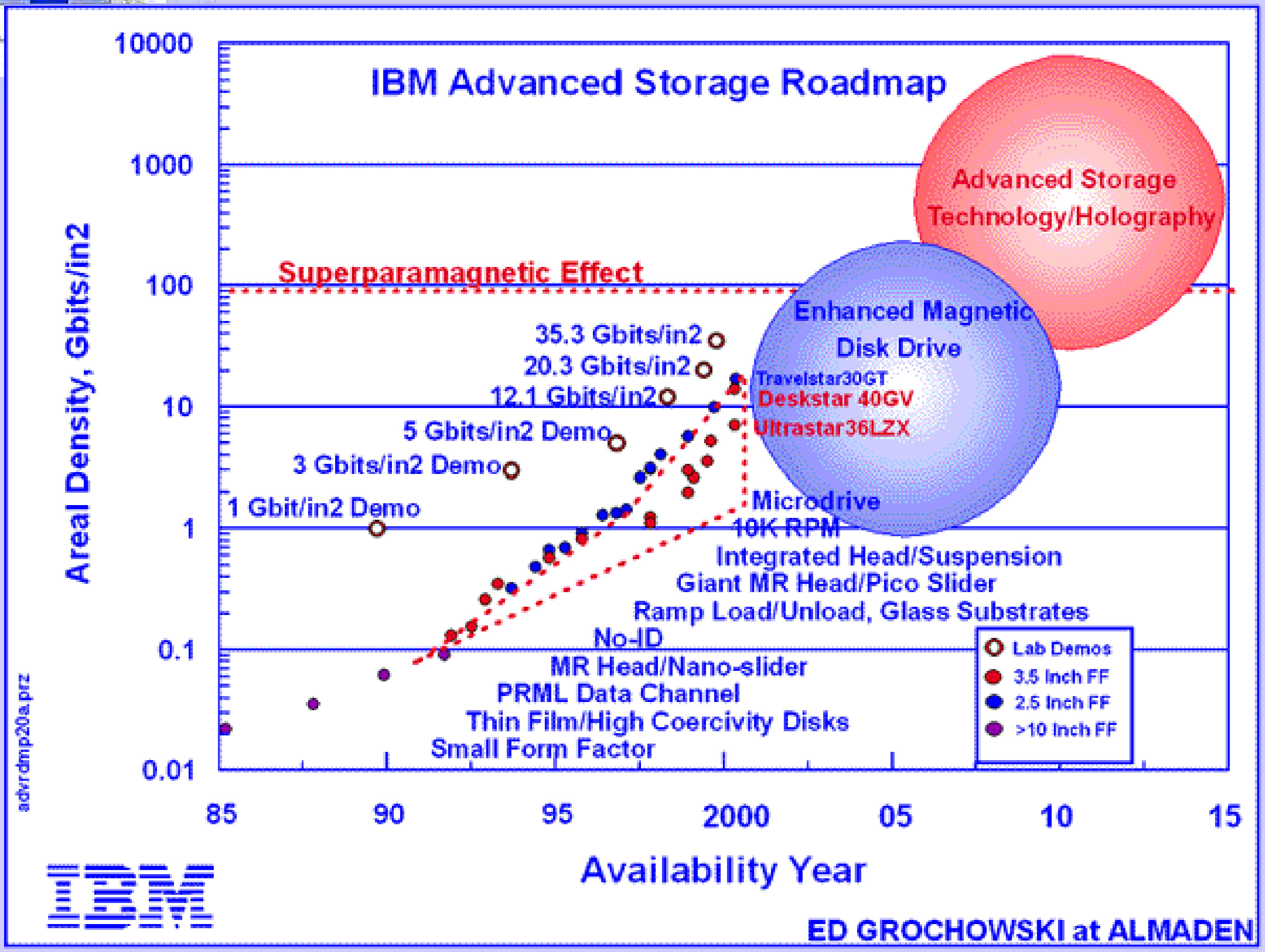

IBM has demonstrated a GMR head with an areal density capability greater than 35.3 billion bits per square inch, and labor

demonstr beyond 5 have been reported, indicating that future disk drives could exhibit capacities at least two times higher than today.

Disk drives will continue to be enhanced through the use of MEMS micro-actuators, fluid bearing spindle motors and even split or multiple actuators. Also, new data storage techniques, as holographic storage are on horizon.

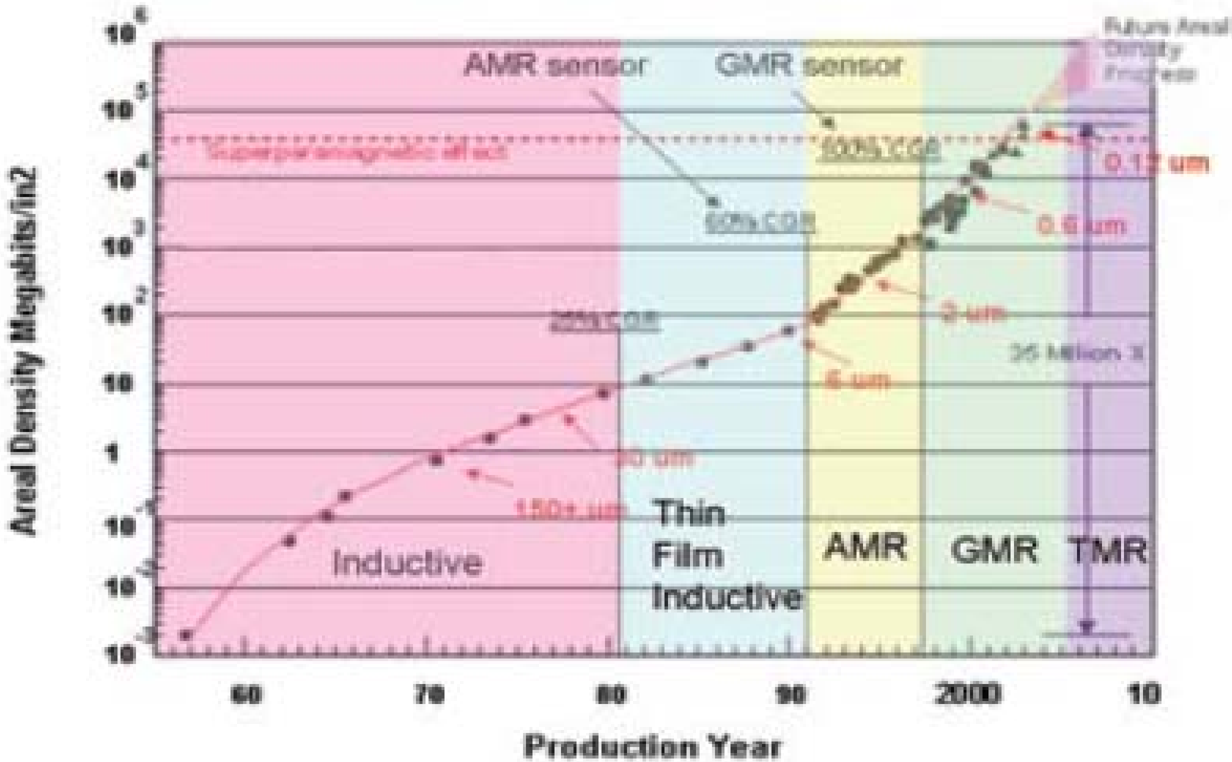

Fig. 7: Magnetic Recording Areal Density vs. year of product introduction, showing the evolution of sensor technologies. The introduction of the GMR spin valve in 1997 is the first commercially successful use of spintronics.

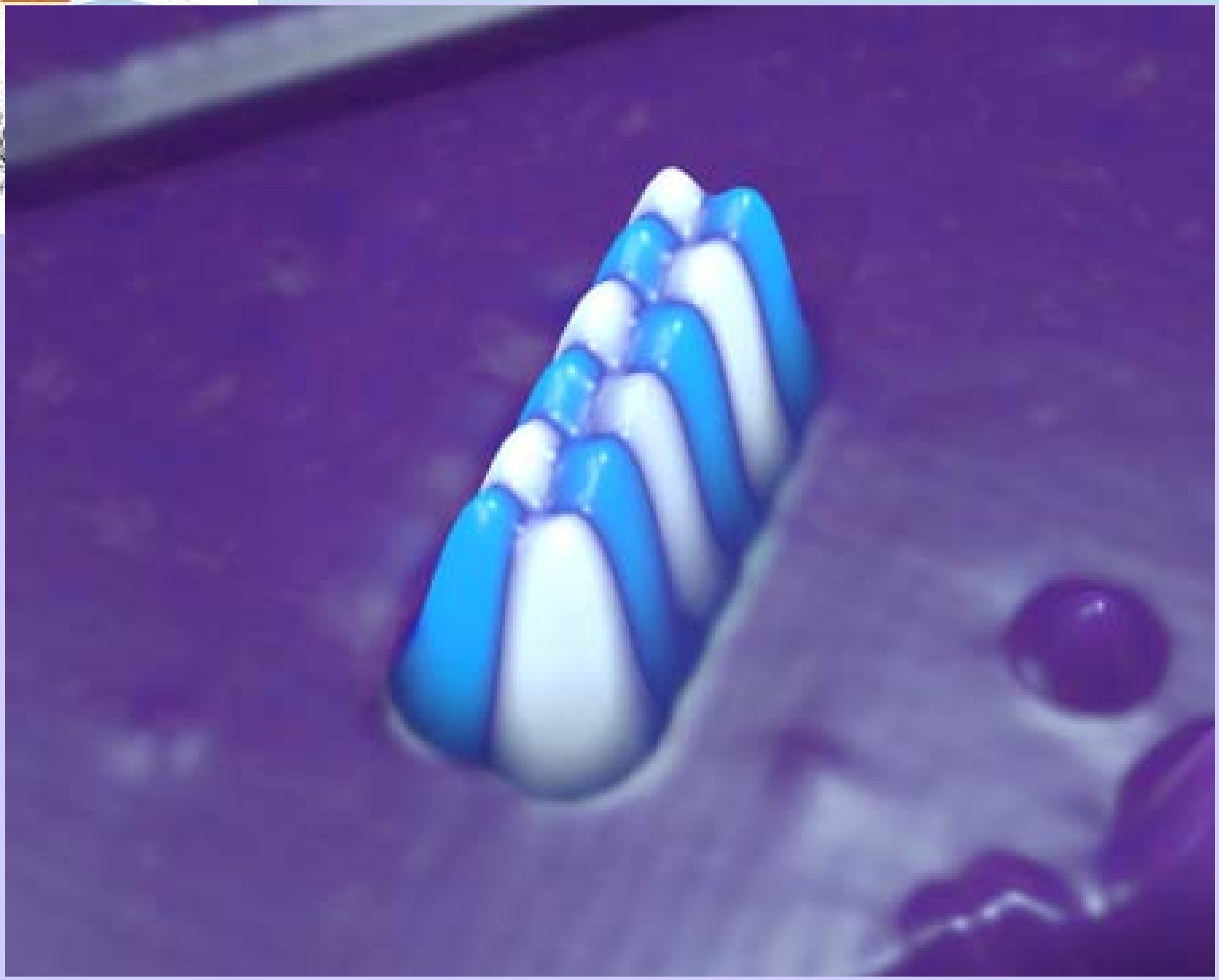

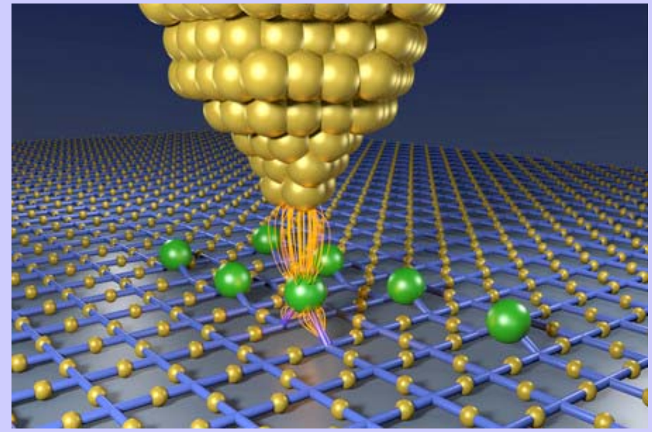

Tunnel microscope manipulation

1 byte =8 bit=96 atoms
Nowaday -10^8 atoms

12 atoms of Fe – artificial antiferomagnet

The smallest magnetic memory cell

↑ ↑ ↑ ↑   ↓ ↓ ↓ ↓
↑ ↓ ↑ ↓   ↓ ↑ ↓ ↑

Electronics, Micro- and Nanoelectronics $\longrightarrow$ Charge of Electron

SPINTRONICS= SPIN+TRANSPORT+ELECTRONICS (1992)

Spintronics $\longrightarrow$ Charge + Spin of Electron

Spin control and manipulation

Spin current without dissipation!!!!?

Quantum Computers

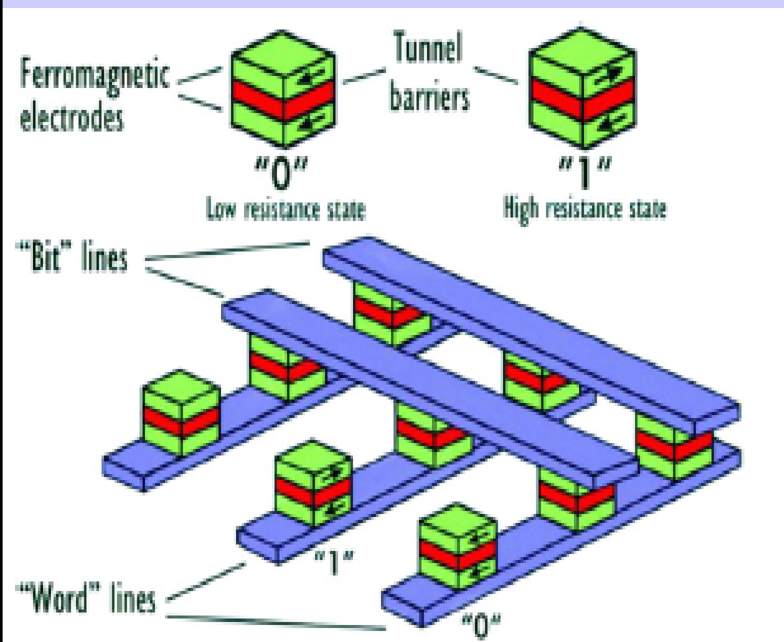

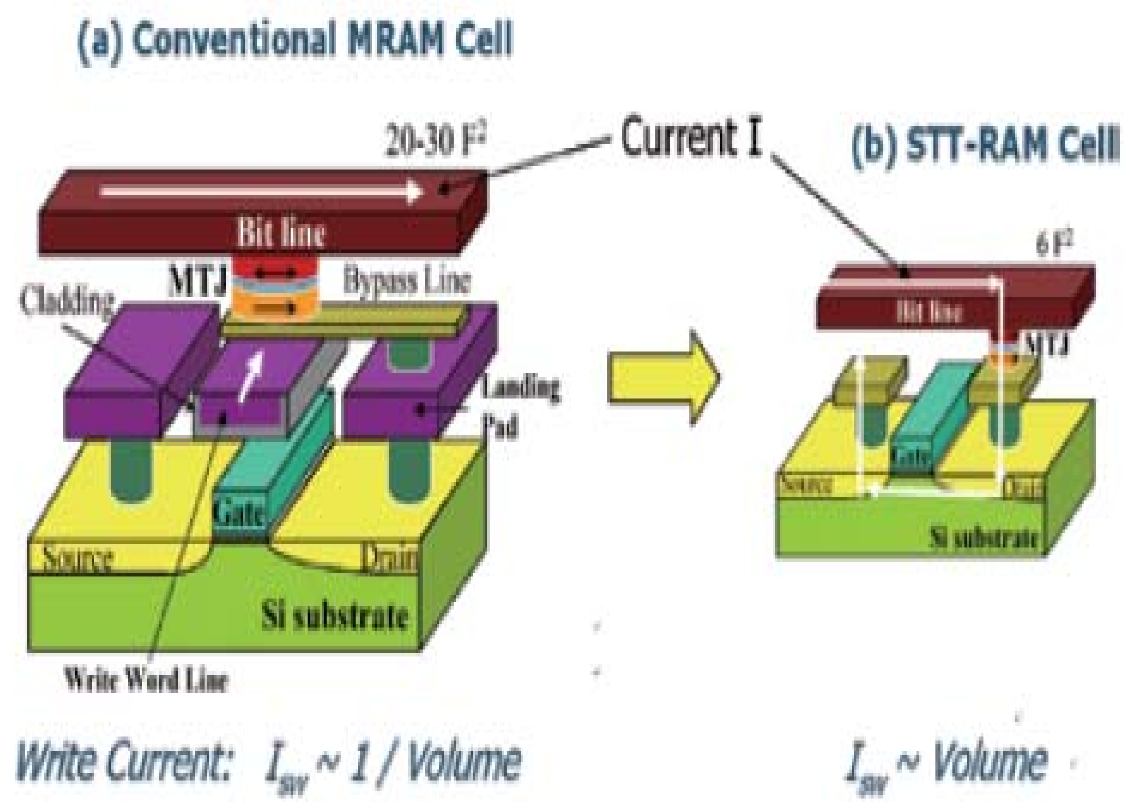

Fig. 1: Comparison of memory cell architecture between conventional field switching MRAM (a) and spin-transfer torque MRAM (STT-MRAM) (b).

Future: From charge current to pure spin current

$$J_e = J_\uparrow + J_\downarrow \quad (1)$$

$$J_s = J_\uparrow - J_\downarrow \quad (2)$$

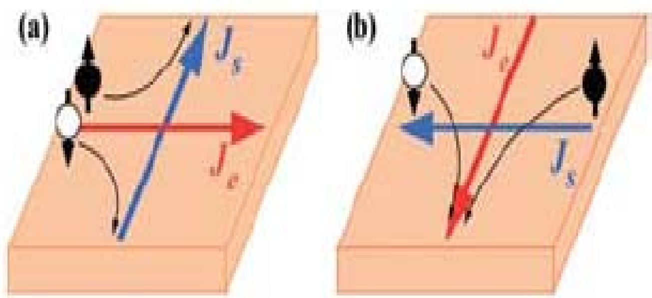

Fig. 6: Schematic illustration of (a) direct and (b) inverse spin-Hall effects in a nonmagnetic material. J_e and J_s are the charge and spin currents, respectively.

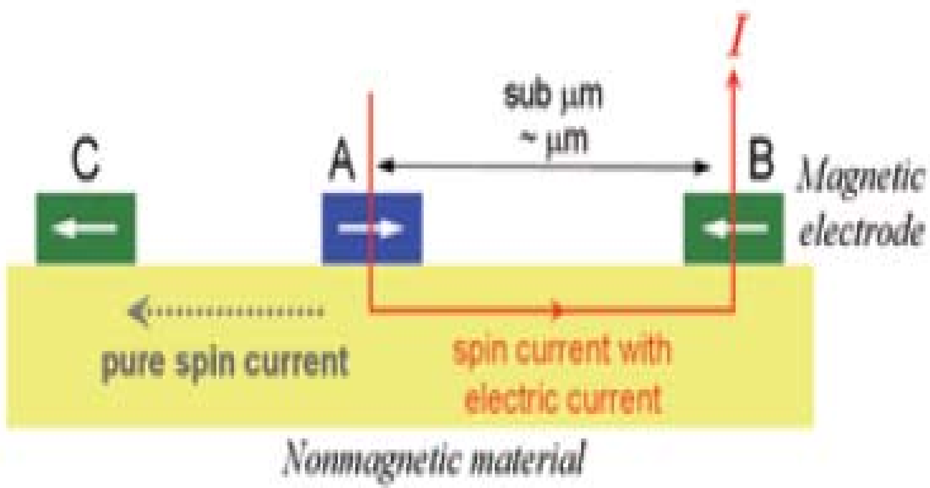

Fig. 1: A basic device structure for the study of spin current.

Spin Hall Effect

Mooij correlation in metals

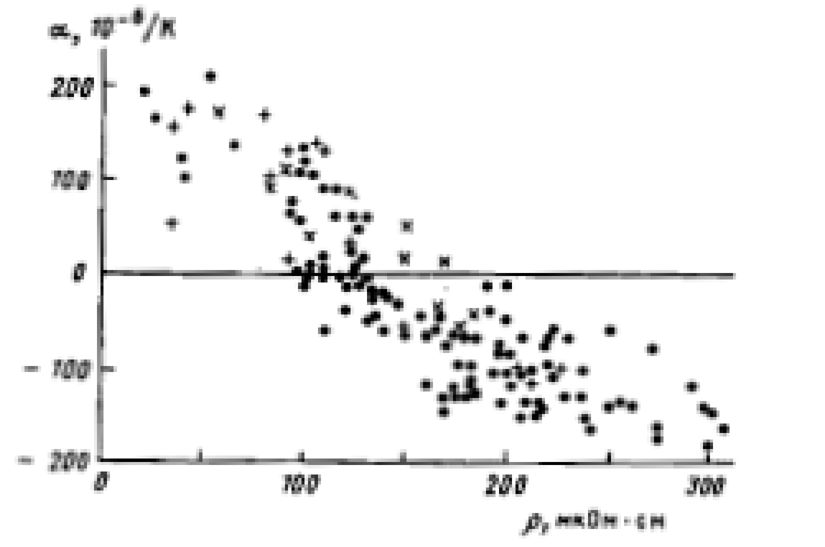

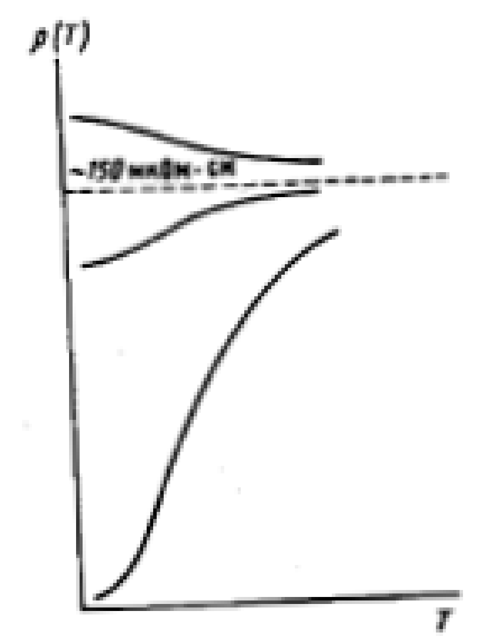

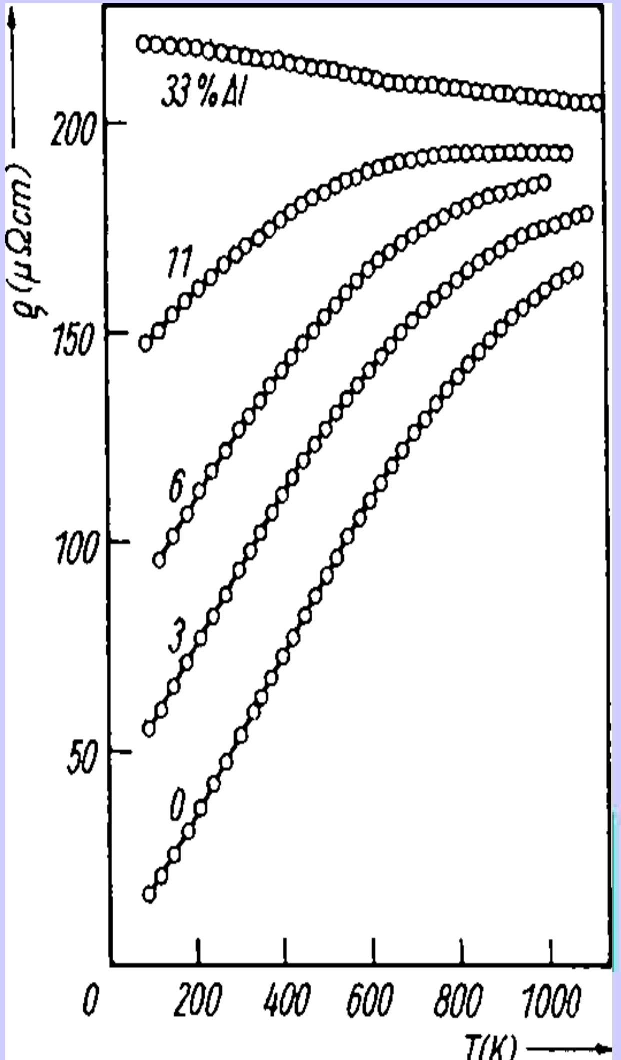

$$\rho = \rho_0 + \rho_1(T), \ \rho_1(T) \ll \rho_0,$$

$$\frac{\partial \rho_1}{\partial T} > 0 \ \text{при} \ \rho_0 < \rho^*,$$

$$\frac{\partial \rho_1}{\partial T} < 0 \ \text{при} \ \rho_0 > \rho^*,$$

Resistivity in ferromagnetic metals

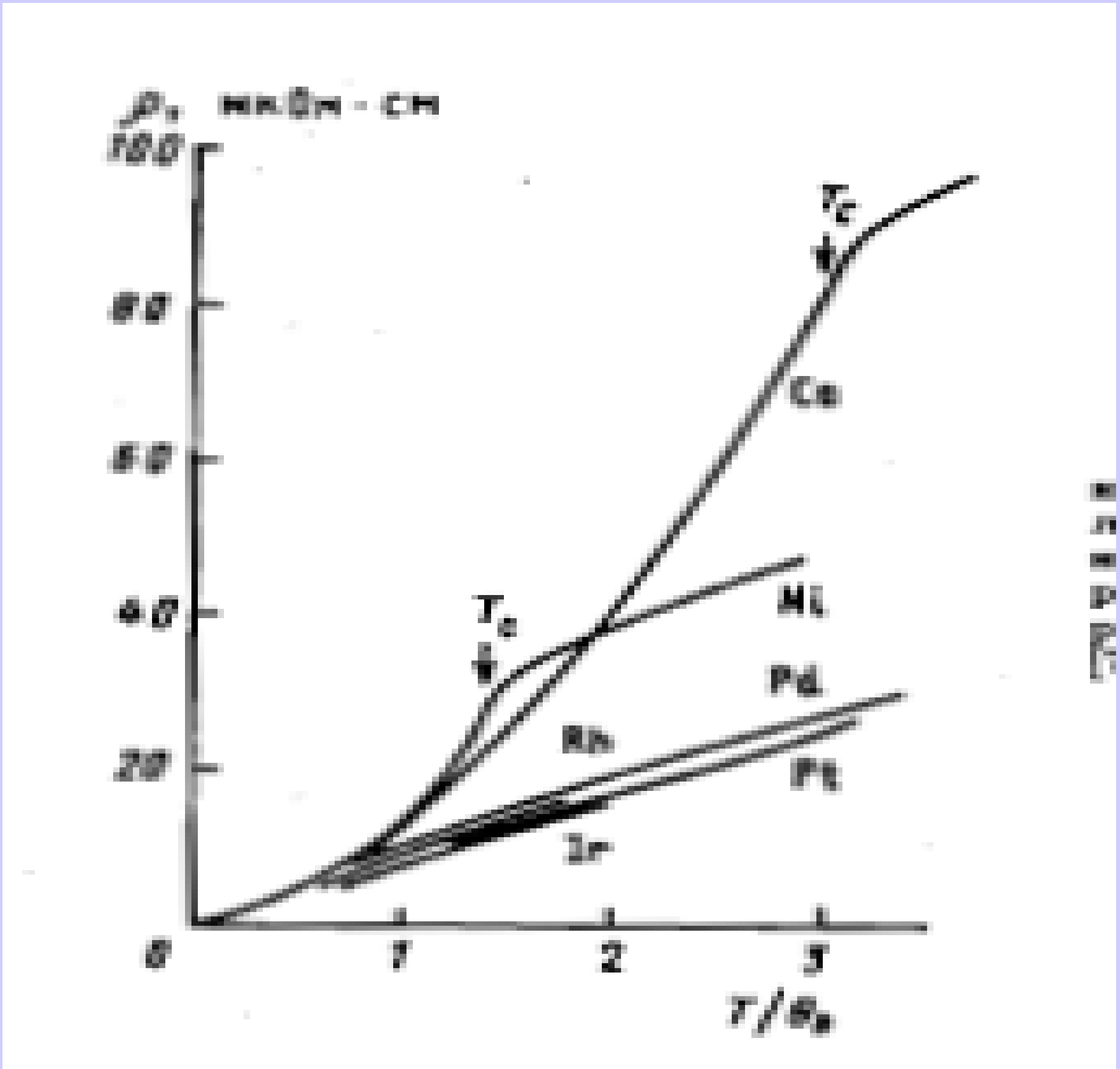

Resistivity: GaAs:Mn

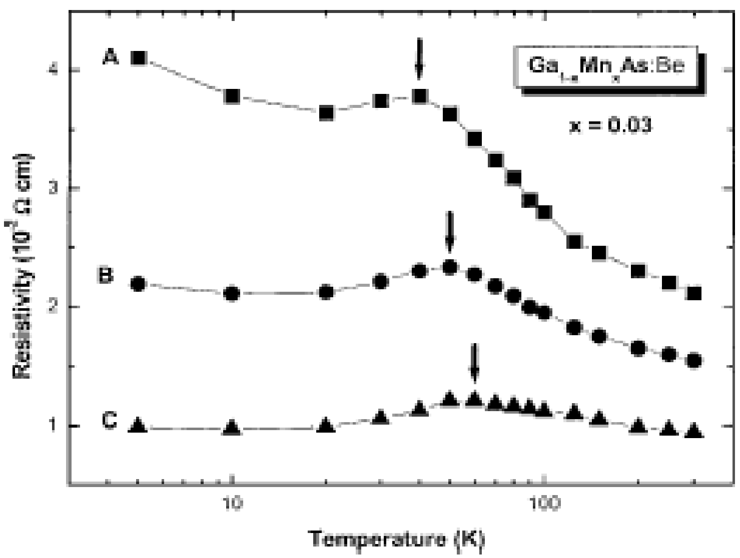

FIG. 1. Temperature dependence of the resistivity for undoped (A) and Be-doped [(B) and (C)] samples of $Ga_{1-x}Mn_xAs$ ($x=0.03$) at zero magnetic field.

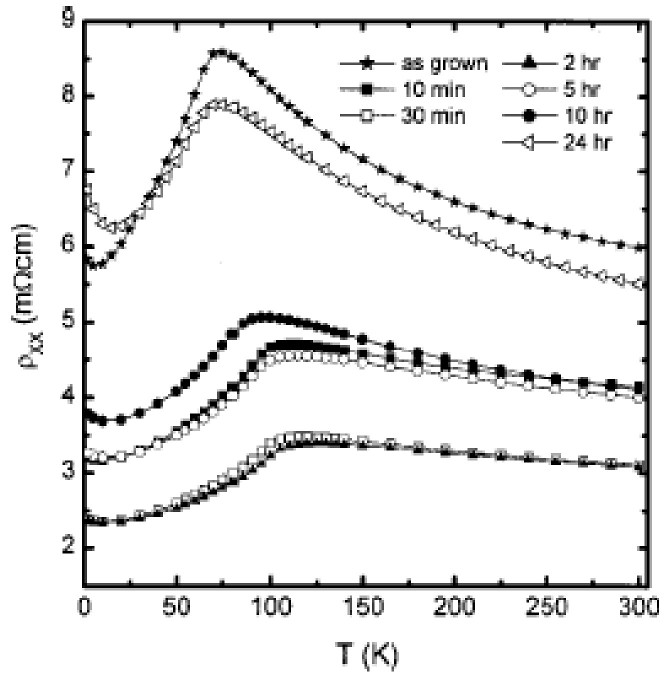

FIG. 38 Experimental resistivity of $Ga_{1-x}Mn_xAs$ for x = 8% vs. temperature for various annealing times. From (Potashnik *et al.*, 2001).

$$\rho = \frac{m^*}{e^2 p \langle \tau_k \rangle} = \frac{e^2 m^{*2} N_I}{8\pi k_F^3 \hbar^3 p \varepsilon_0^2 (1-\Gamma)^2}\left[\ln(1+\alpha) - \frac{\alpha}{1+\alpha}\right],$$

$$\alpha = 4k_F^2 r_s^2,$$

$$\Gamma \approx \frac{J_{pd}^4 S^2 (S+1)^2 m^* N^2 k_F p}{4\pi^2 E_F^2 \hbar^2 k_B T}\left[1 - \frac{3k_F a}{4\pi}\right],$$

See, reviews of T. Jungwirth

Resistivity in TiO_2:Co

$$\sigma = \sigma_0 \exp(-E_a/kT)$$

$$\sigma = \sigma_0 \exp(-T_0/T)^s$$

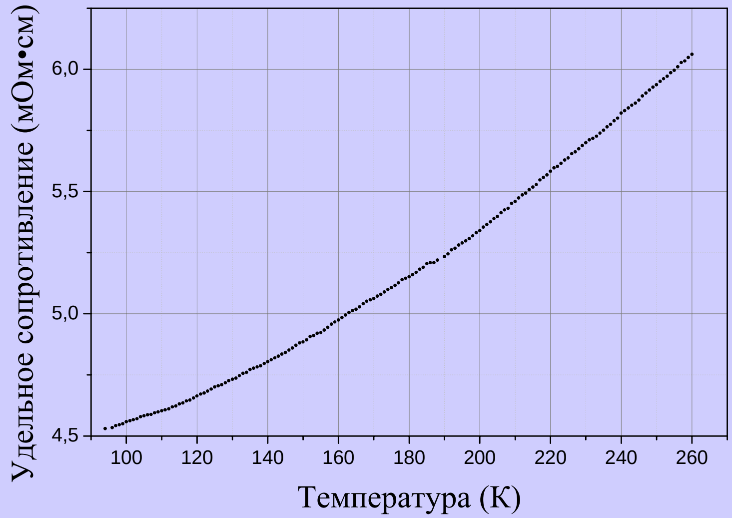

s=1/4 Mott (VRH)
s=1/2 Efros-Shklovski (VRH + Gap)
s=1 Activation

Yu. Mikhailovski

SPH =small polaron hopping ($T>\Theta_D/4$)

$$\sigma = \sigma_0 T^{-\alpha} \exp(-W/kT)$$

A.Yildis et al. JAP 2010

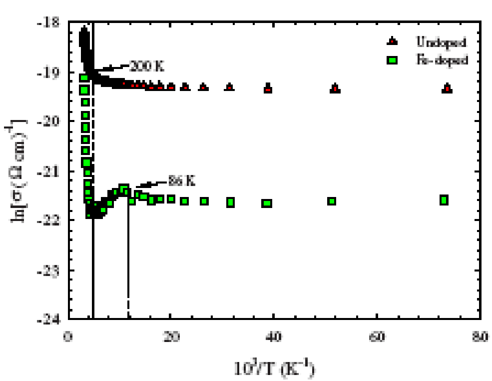

FIG. 2. (Color online) Temperature dependence of the conductivity plotted as $\ln(\sigma)$ vs $10^3/T$ in the temperature range 13–320 K.

1856
Thompson

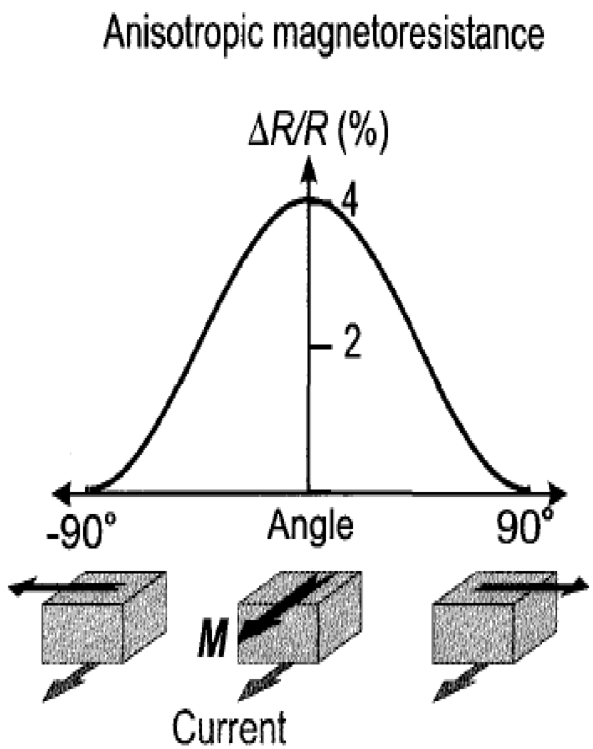

Permalloy: AMR=4-5% at 300 K, H=5 Oe

$$\frac{MR,\%}{H} = 1\%/Oe$$

$$\rho_{ij} = \begin{vmatrix} \rho_\perp(B) & -\rho_H(B) & 0 \\ \rho_H(B) & \rho_\perp(B) & 0 \\ 0 & 0 & \rho_\parallel(B) \end{vmatrix}$$

$$\frac{\Delta\rho}{\rho} = \frac{\rho_\parallel - \rho_\perp}{\frac{1}{3}\rho_\parallel + \frac{2}{3}\rho_\perp}.$$

$$\vec{E} = \rho_\perp(B)\vec{j} + [\rho_\parallel(B) - \rho_\perp(B)](\vec{\alpha}\cdot\vec{j})\cdot\vec{\alpha} + \rho_H(B)[\vec{\alpha} \times \vec{j}],$$

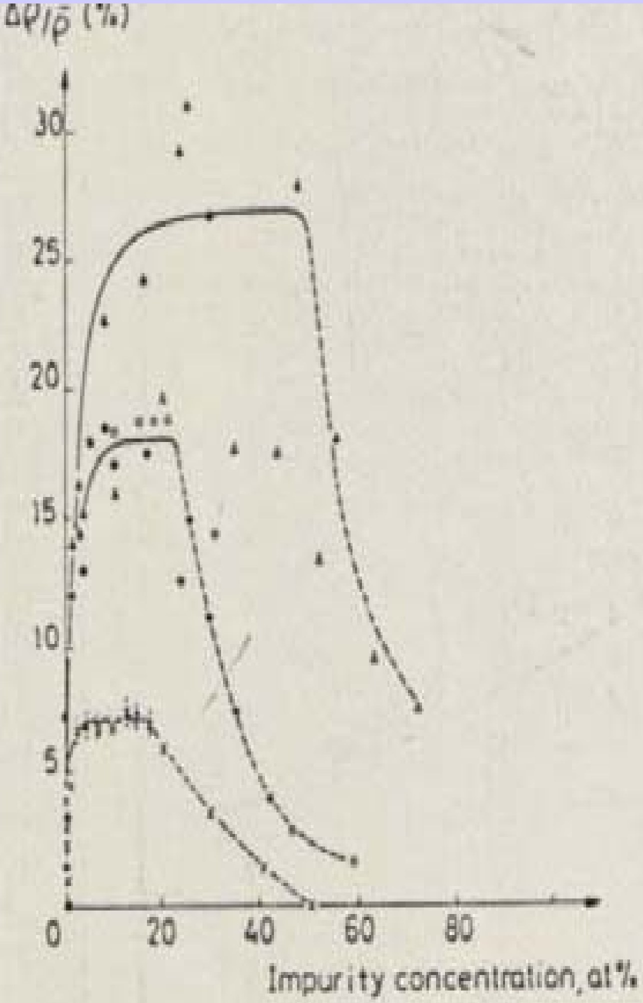

Fig. 13. Concentration dependence of the resistivity anisotropy at 4.2 K for several nickel based alloys. ▲△: NiCo, ●○: NiFe, ×: NiCu (after Jaoul et al. 1977).

$\Delta\rho/\rho = 0.01(\alpha - 1)$

$\alpha = \rho_{\downarrow}/\rho_{\uparrow}$

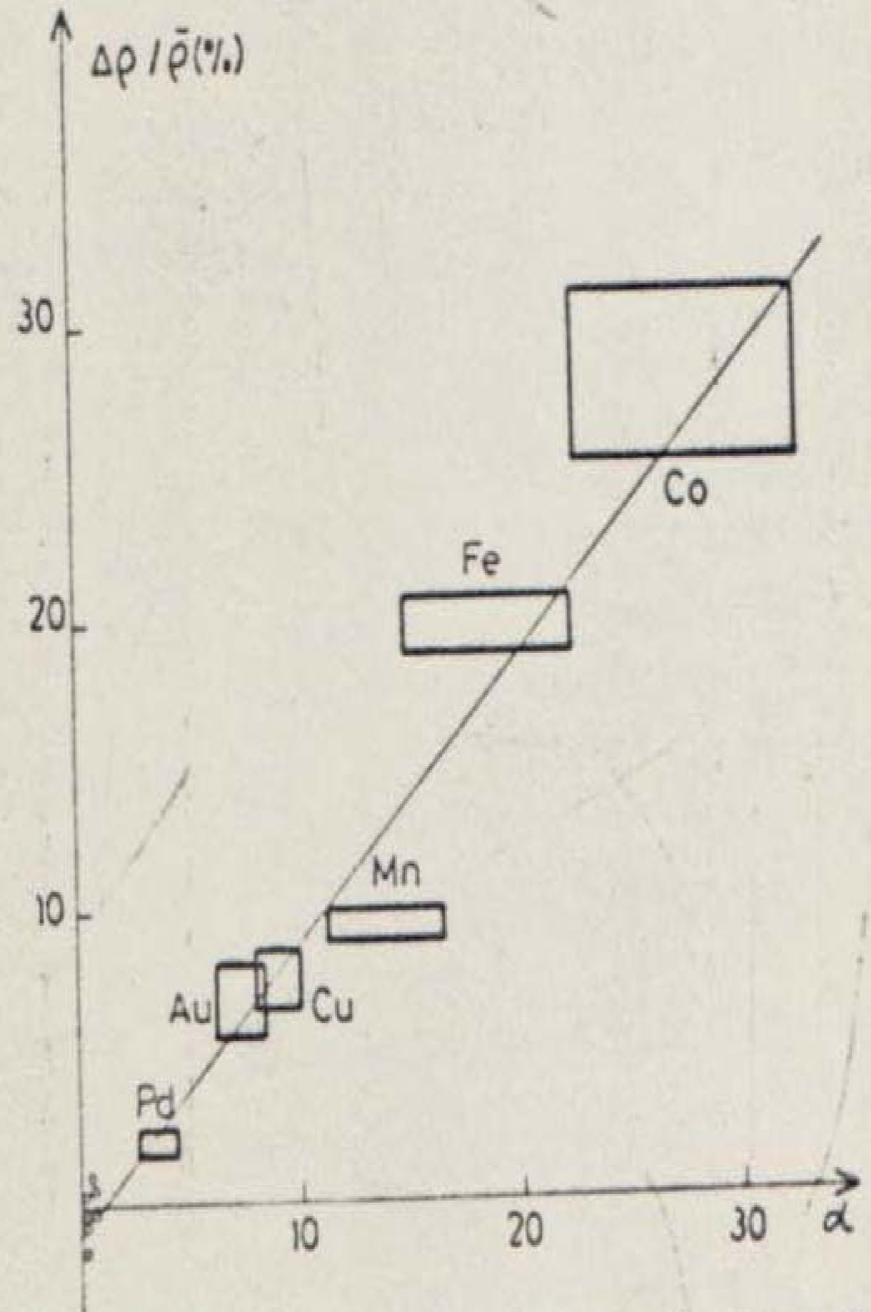

Fig. 14. Resistivity anisotropy of Ni based alloys at 4.2 K as a function of $\alpha = \rho_{0\downarrow}/\rho_{0\uparrow}$. The straight line is $\Delta\rho/\bar{\rho} = 0.01\ (\alpha - 1)$ (after Jaoul et al. 1977).

AMR in GaAs:Mn

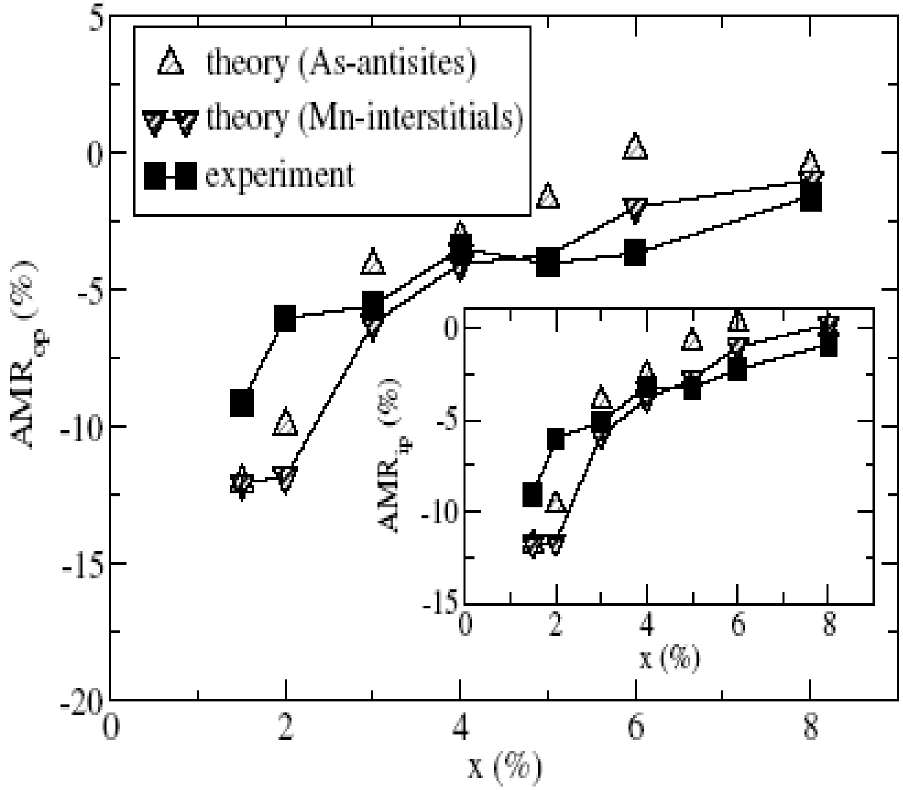

Fig. 3. Experimental (filled symbols) AMR coefficients and theoretical data obtained assuming As-antisite compensation (open symbols) and Mn-interstitial compensation (semi-filled symbols) of AMR_{op} and AMR_{ip}. (After Ref. 52.)

No data in TiO2:Co

2009

Novel types of magnetoresistance

Giant magnetoresistance in semiconductor / granular film heterostructures with cobalt nanoparticles

L.V. Lutsev[1], A.I. Stognij[2], and N.N. Novitskii[2]

In this paper, we study the magnetoresistance in SiO_2(Co)/GaAs and SiO_2(Co)/Si heterostructures, where the SiO_2(Co) is the granular SiO_2 film with Co nanoparticles. Sample preparation and experimental results are presented in section 2. The effect is more expressed, when electrons are injected from the granular film into the SC, therefore, the magnetoresistance has been called the injection magnetoresistance (IMR) [38, 39]. For SiO_2(Co)/GaAs heterostructures the IMR value r of the magnetoresistance effect in perature, which is two-three orders higher than maximum valu by magnetic-field-controlled pro- c multilayers and the TMR in MTJ structures. On the contrary, for SiO_2(Co)/Si heterostructures the magnetoresistance

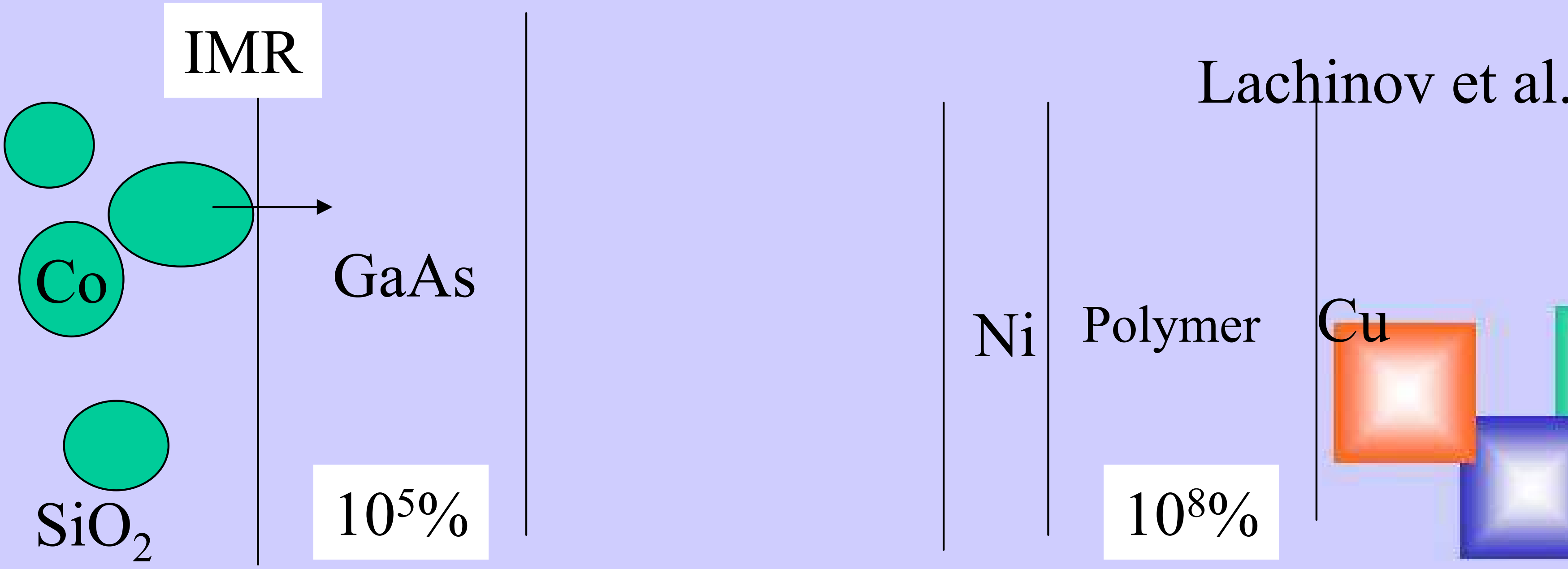

Magnetism Department, Faculty of Physics, MSU

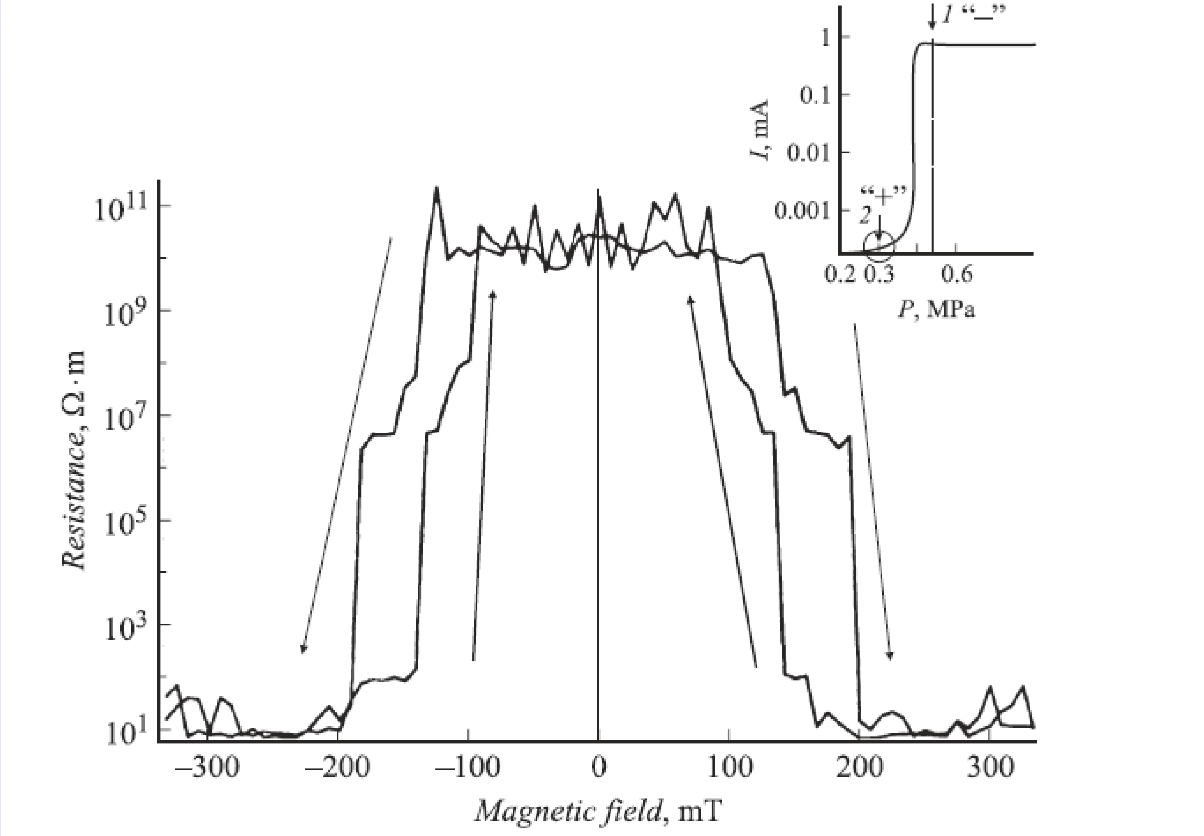

Ni-polymer-Cu

800 nm

Lachinov 2009

ORGANIC MAGNETORESISTANCE

Francis 2004

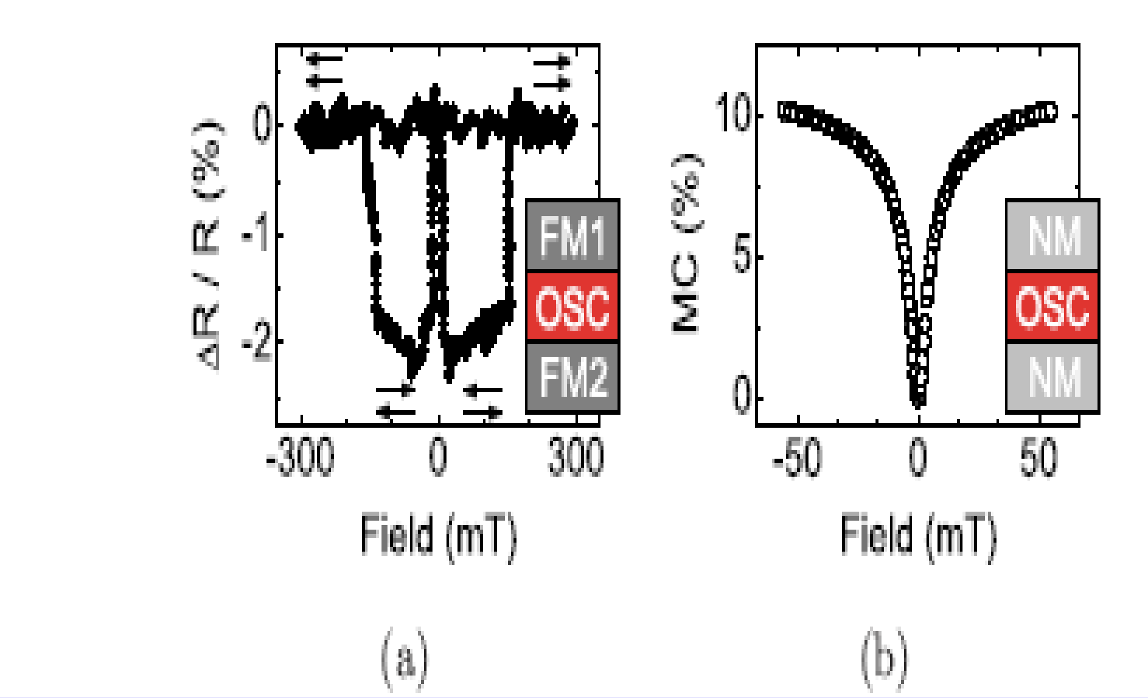

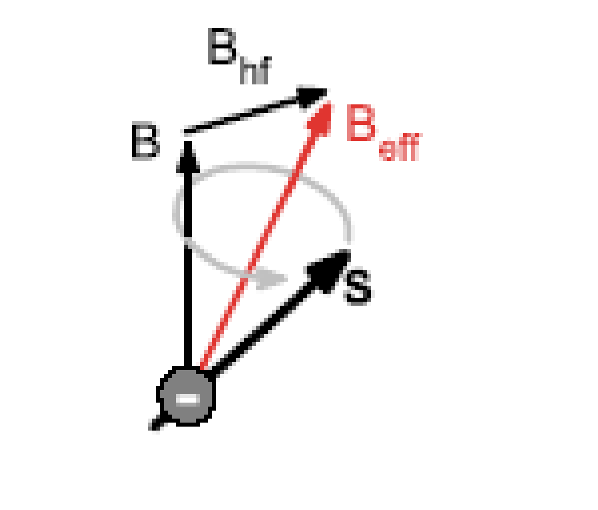

W. Wagemans et al. SPIN, vol.1. no.1 p.94 (2011)

Ordinary Hall effect

$$\rho_{xy} = R_0 B$$

Anomalous Hall effect

$$\rho_{xy} = R_0 B + \rho_{ah}$$

$$\rho_{ah} = 4\pi M_z$$

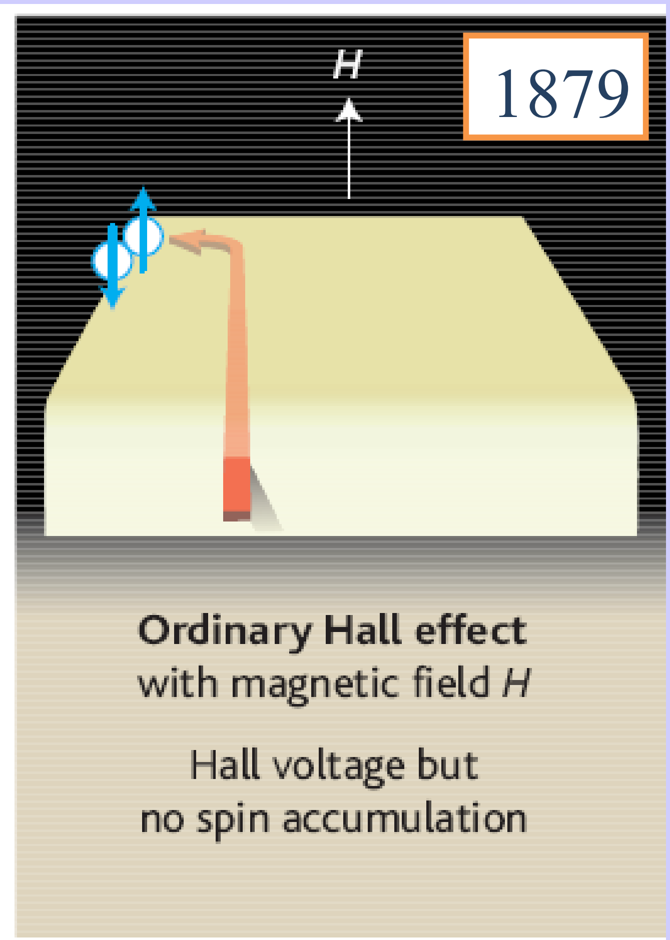

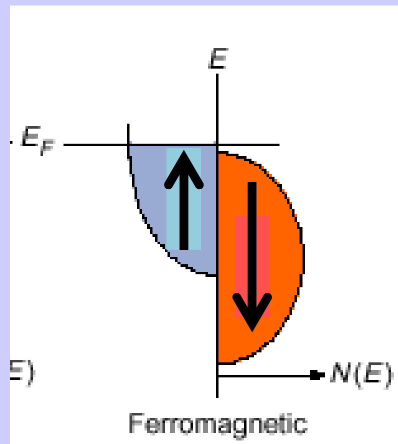

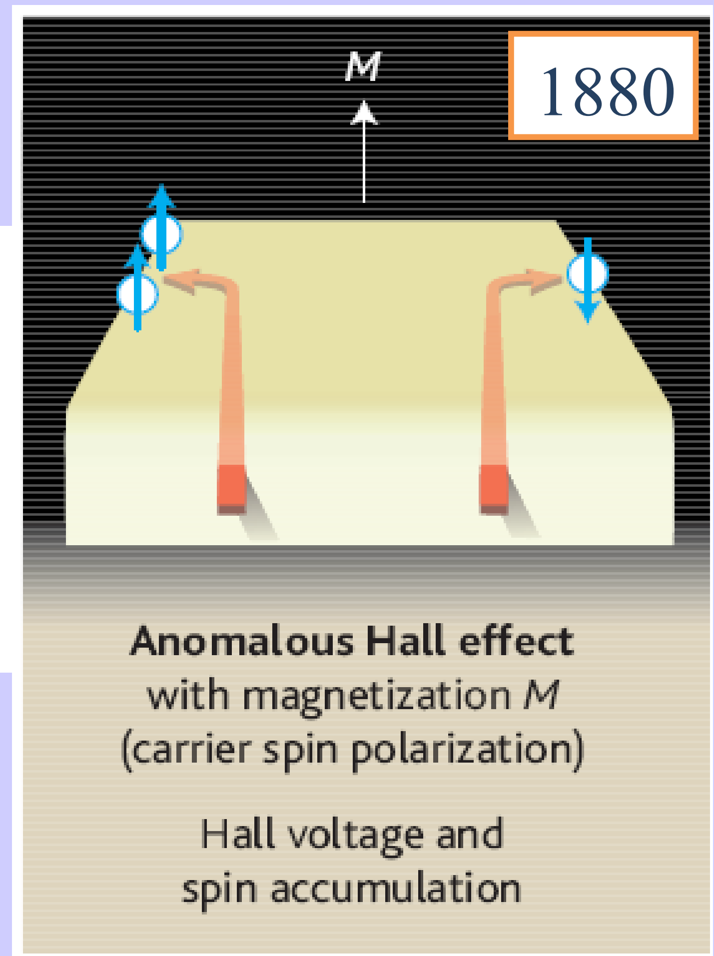

Lorentz Force

$$B = H + 4\pi M(1-N)$$

Spin-Orbit Coupling

Spin-orbit coupling

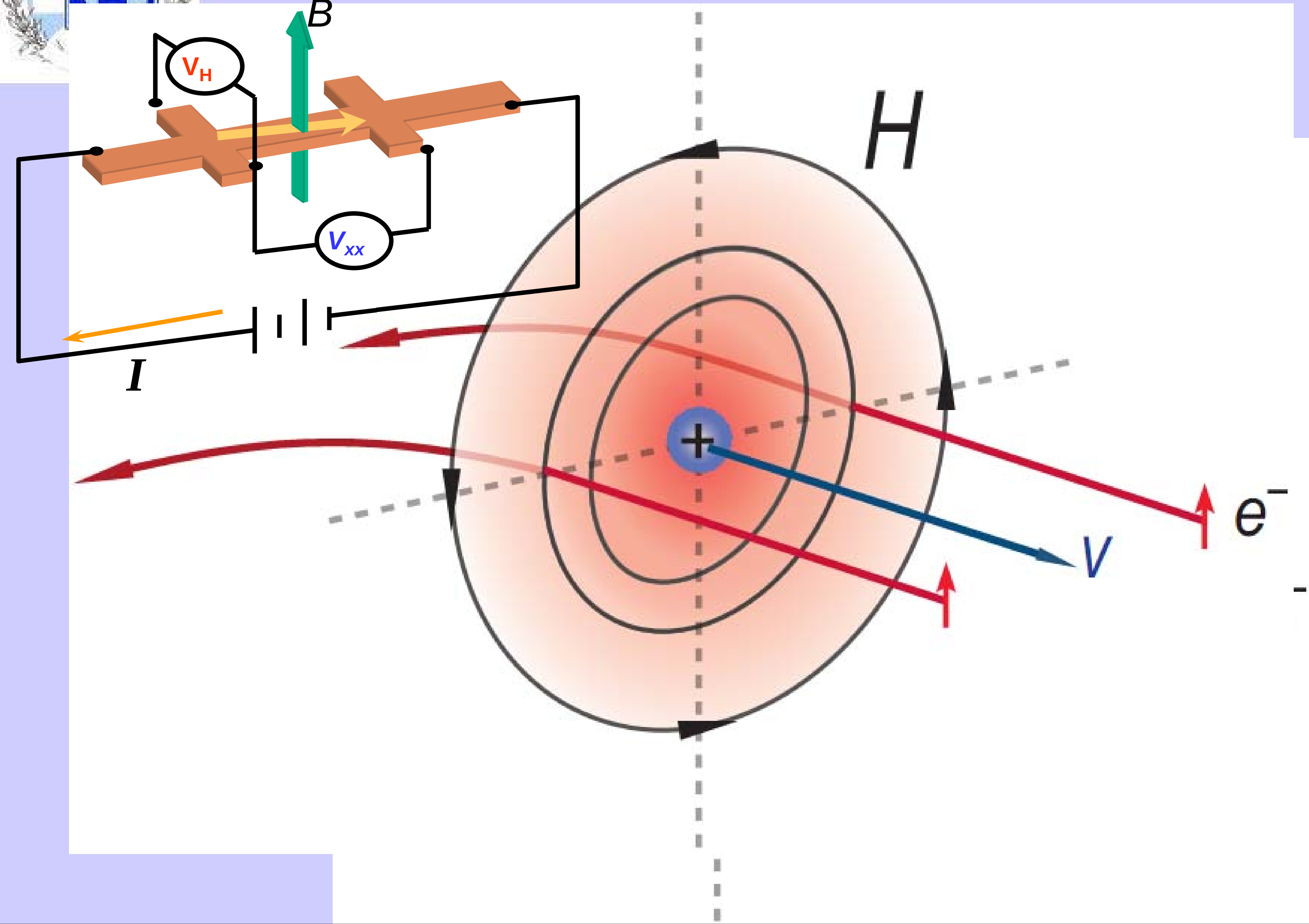

Hall Effect

$$\rho_H = R_0 B_z + 4\pi R_s M_z$$

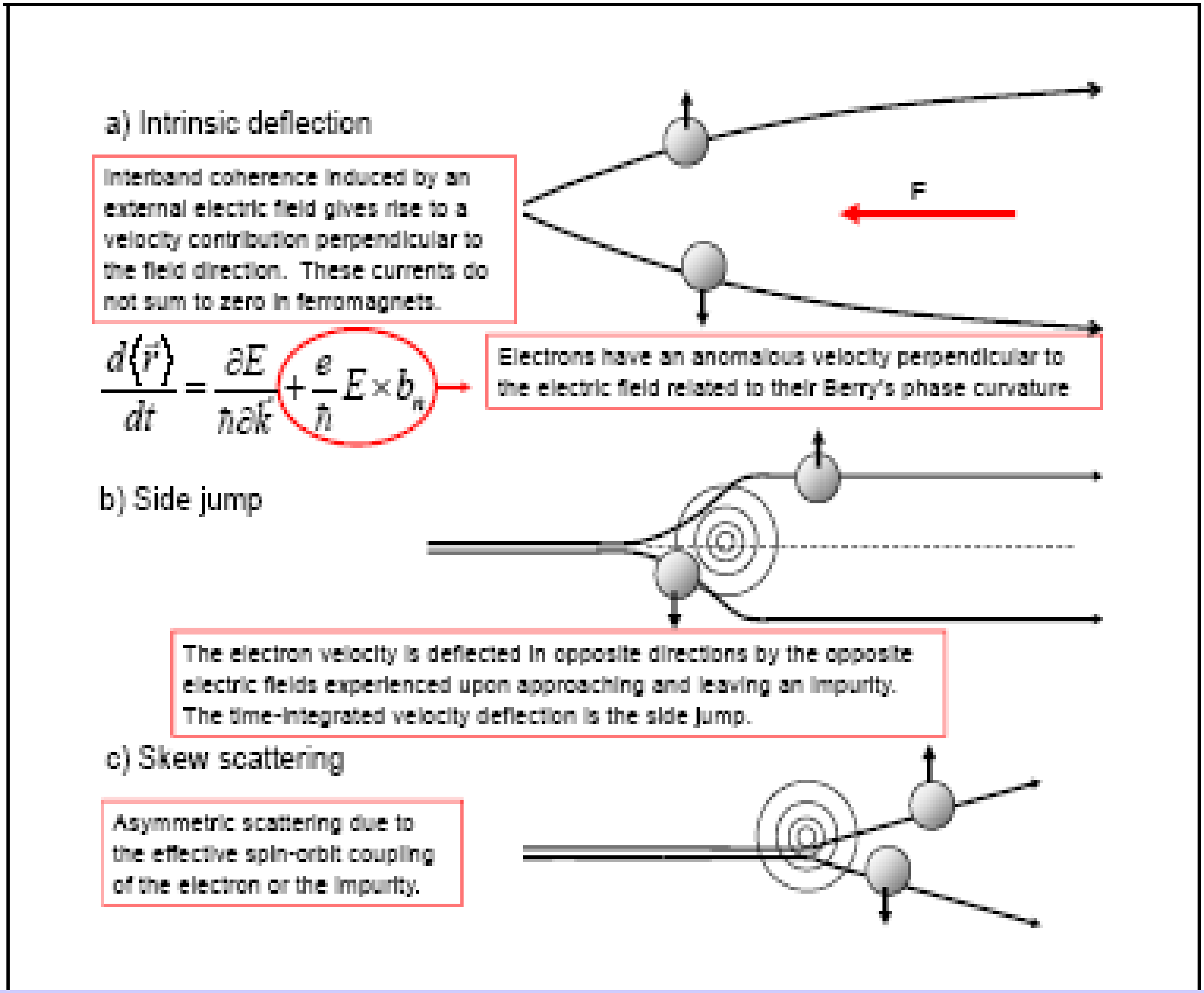

Nagaosa et al.

(1) Karplus-Luttinger Intrinsic (1954)

Anomalous velocity

$$\frac{d\vec{r}(t)}{dt} = \frac{\partial \varepsilon_n(\vec{k})}{\partial \vec{k}} - \vec{\Omega}_n(\vec{k}) \times \frac{d\vec{k}(t)}{dt}$$

k- space curvature

$$\frac{d\vec{k}(t)}{dt} = \frac{\partial V(\vec{r})}{\partial \vec{r}} - \vec{B}(\vec{r}) \times \frac{d\vec{r}(t)}{dt}$$

r- space curvature

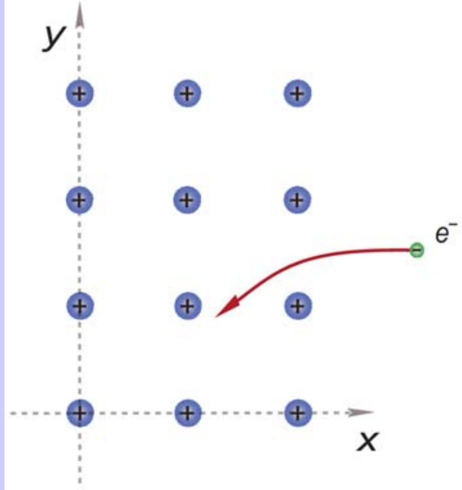

G. Sundaram and Q. Niu,
Phys. Rev. B 59 (1999) 14915.

Jungwirth, Niu, MacDonald (2002), Onoda & Nagaosa (2002)

$$\sigma_{xy} = -\frac{e^2}{\hbar}\int d^3\mathbf{k}\sum_n f(\varepsilon_n(\mathbf{k}))\boxed{\Omega_n^z(\mathbf{k})}$$

Berry curvature

$$\Omega_n^z(\mathbf{k}) = -\sum_{n'\neq n}\frac{2\,\mathrm{Im}\langle \mathbf{k}n|v_x|\mathbf{k}n'\rangle\langle \mathbf{k}n'|v_y|\mathbf{k}n\rangle}{(\omega_{\mathbf{k}n'}-\omega_{\mathbf{k}n})^2}$$

$$\sigma_{\text{int}} = constant \longrightarrow \rho_{\text{int}} = \sigma_{\text{int}}\rho_{xx}^2$$

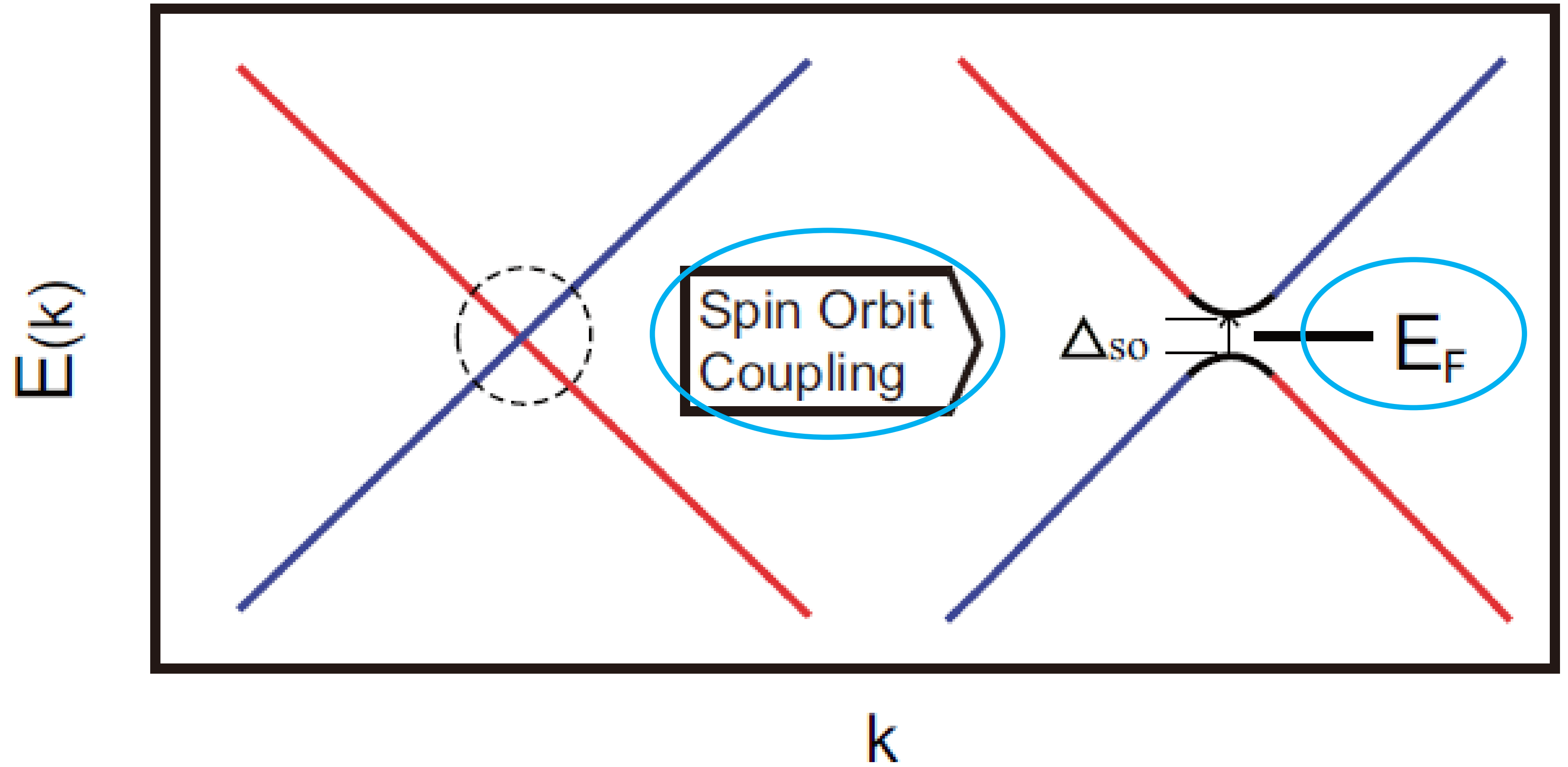

$$\Omega_n^z(\mathbf{k}) = -\sum_{n'\neq n} \frac{2\,\mathrm{Im}\langle \mathbf{k}n | v_x | \mathbf{k}n'\rangle\langle \mathbf{k}n' | v_y | \mathbf{k}n\rangle}{(\omega_{\mathbf{k}n'} - \omega_{\mathbf{k}n})^2}$$

S. Onoda, N. Sugimoto, N. Nagaosa, PRL, 97, 126602 (2006)

(2) Skew-scattering (Smit, 1955)

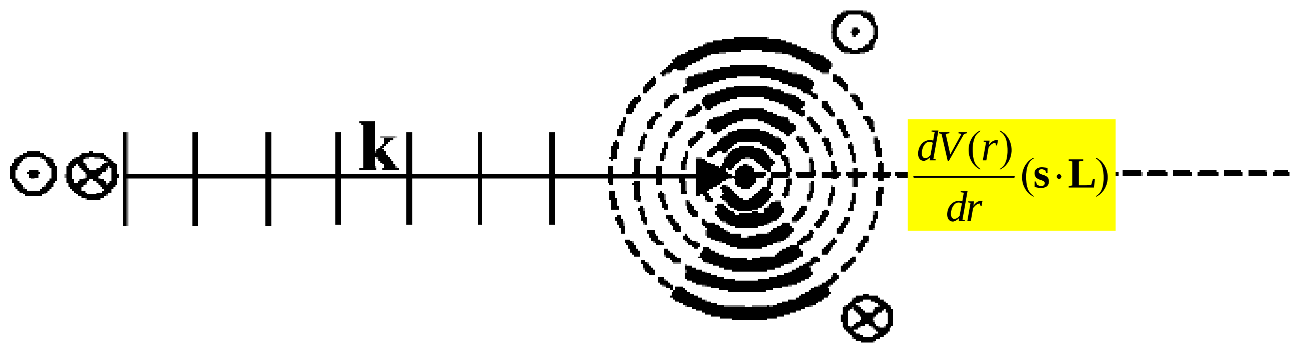

$$\rho_{ah} = \alpha \rho_{xx}$$

c«1
(T=0)

(3) Side-jump (Berger, 1970)

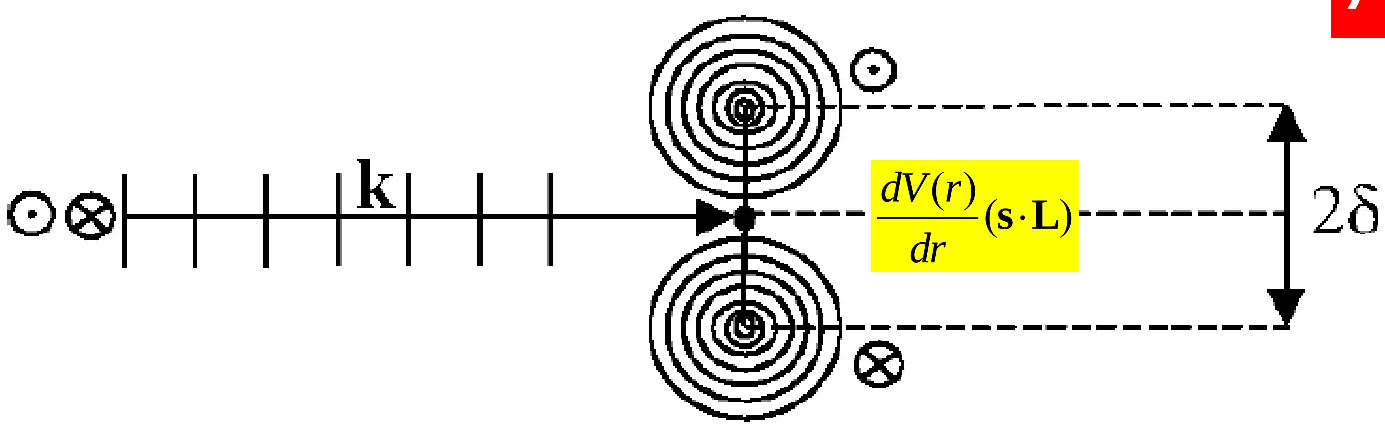

$$\rho_{ah} = \beta \rho_{xx}^2$$

$$\rho_{ah} = a\rho_{xx} + b\rho_{xx}^2$$

Intrinsic or Extrinsic ?!

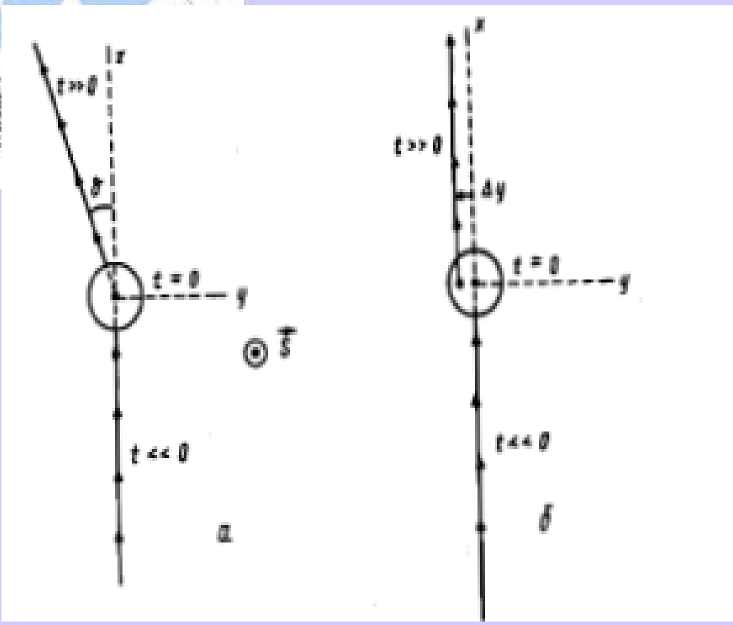

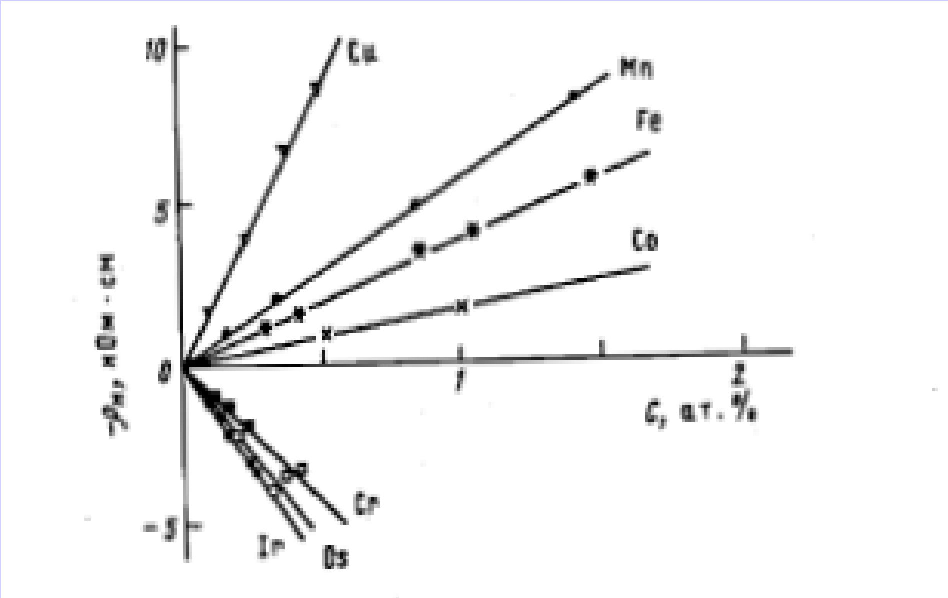

Size-effects
Weak localization
Electron-electron interaction
Short –range order

No doubt that at T=0 and low impurity concentration AHE is due to skew scattering

$$(R_s)^{sc} = a\rho_0 + b\rho_0^2$$

Only T=0 and low impurity concentration

Intrinsic and Extrinsic ?

$$\rho_{ah} = a\rho_{xx} + b\rho_{xx}^2$$

$$\rho_{ah} = \underbrace{\alpha\rho_{xx0} + \beta\rho_{xx0}^2}_{\text{Extrinsic}} + \underbrace{b\rho_{xx}^2}_{\text{Intrinsic}}$$

Jin et al. 2012 –ICM2012

Skew scattering for disordered alloys at T=0

$$R_s = c(1-c)(1-2c+f)$$

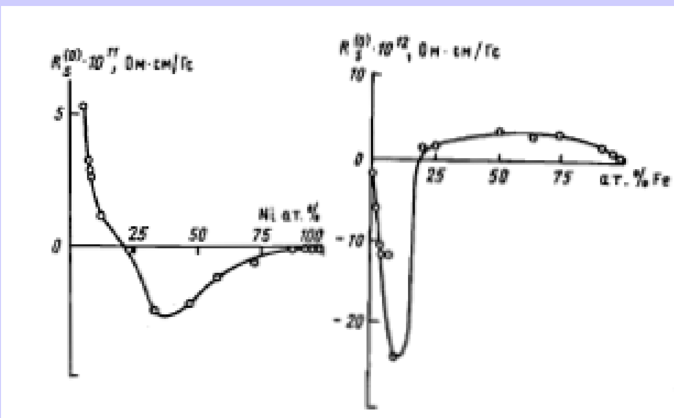

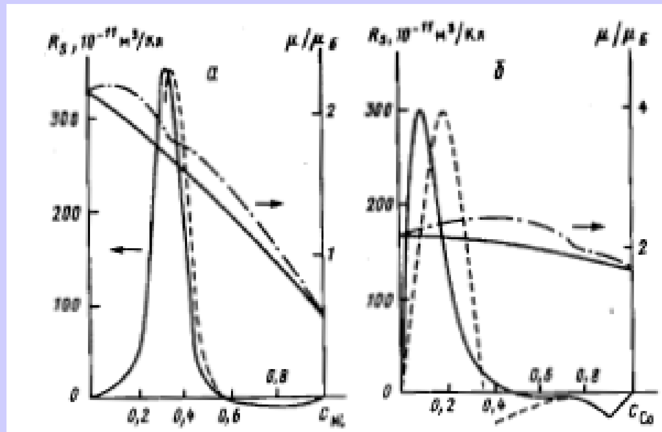

Рис. 25. Концентрационная зависимость коэффициента остаточного АЭХ и намагниченности железо-никелевых (а) и железо-кобальтовых (б) сплавов (сплошные кривые – расчетные данные, пунктирные – экспериментальные) [171]

Nagaosa

$$(R_s)^{sc} = a\rho_0 + b\rho_0^2$$

<1 μΩcm

ρ

$$(R_s)^{KL} = A\rho^2 \qquad (R_s)^{sj} = B\rho^2$$

<100 μΩcm

$$(R_s) = D\rho^{0.4-0.2} \qquad (\sigma_{xy}) \propto \sigma_{xx}^{1.6-1.8}$$

>100 μΩcm

AEH in hopping

$$(\sigma_{xy}) \propto \sigma_{xx}^{1.5}$$

A.Vedyaev and A.Granovsky, Phys. Solid State **28**, 2310 (1986).

size [6], we derive the parametric relationship between the Hall ρ_h and the longitudinal ρ_{xx} resistivities (the parameter is temperature): $\rho_h \propto \rho_{xx}^m$; $m \approx 0.6$. This relationship fits the experimental results well.

JETP Lett. 2000

Magnetism Department, Faculty

ELSEVIER

Journal of Magnetism and Magnetic Materials 136 (1994) 229–232

Journal of magnetism and magnetic materials

Extraordinary Hall effect (EHE) of ferromagnetic composites in the effective medium approximation

A.B. Granovsky [a,*], A.V. Vedyayev [a], F. Brouers [b]

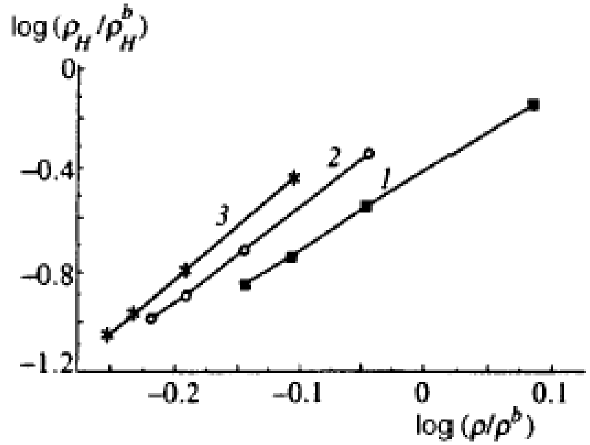

FIG. 2. Correlation between the Hall resistivity ρ_H/ρ_H^b and total resistivity ρ/ρ^b of a granular alloy, having the form $(\rho_H/\rho_H^b)\sim(\rho/\rho^b)^n$; $c=0.2$, $p_b=0.2$, $p_s=0.52$, $l_{m(s)}=120$ Å, $l_{m(d)}=20$ Å, $l_{nm}=200$ Å, $\rho_H^s/\rho_H^b=1$, $r_0=20-80$ Å. The power n depends on the nature of scattering by the surfaces of the grains: $l_s/a_0=2$, $n=3.1$ (curve *1*); $l_s/a_0=4$, $n=3.8$ (curve *2*); $l_s/a_0=6$, $n=4.3$ (curve *3*).

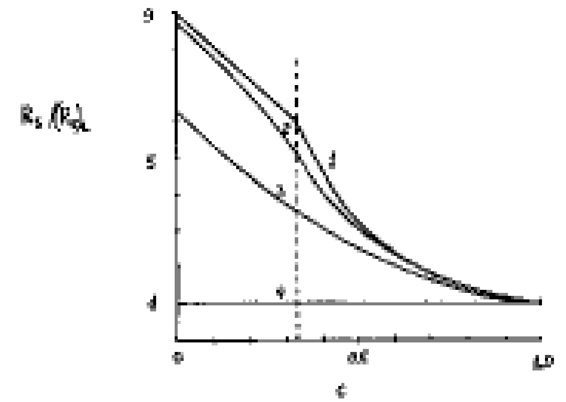

Fig. 1. Reduced EHE coefficient $R_s/(R_s)_1$ for composites versus the concentration x of the ferromagnetic component ($(R_s)_2=0$, $M=xM_1$): 1, $\alpha=\sigma_2/\sigma_1=0$; 2, $\alpha=10^{-2}$; 3, $\alpha=10^{-1}$; 4, $\alpha=1$.

$$\rho_H=\frac{x}{x+y\left(\frac{\rho_2}{\rho_1}\right)^2\left(\frac{\rho+2\rho_1}{\rho+2\rho_2}\right)^2}\left[R_{0\,1}B_1+4\pi R_{s\,1}M_1\right]\left(\frac{\rho}{\rho_1}\right)^2+$$

$$+\frac{y}{y+x\left(\frac{\rho_1}{\rho_2}\right)^2\left(\frac{\rho+2\rho_2}{\rho+2\rho_1}\right)^2}\left[R_{0\,2}B_2+4\pi R_{s\,2}M_2\right]\left(\frac{\rho}{\rho_2}\right)^2$$

Giant Hall effect in NiFe-SiO_2

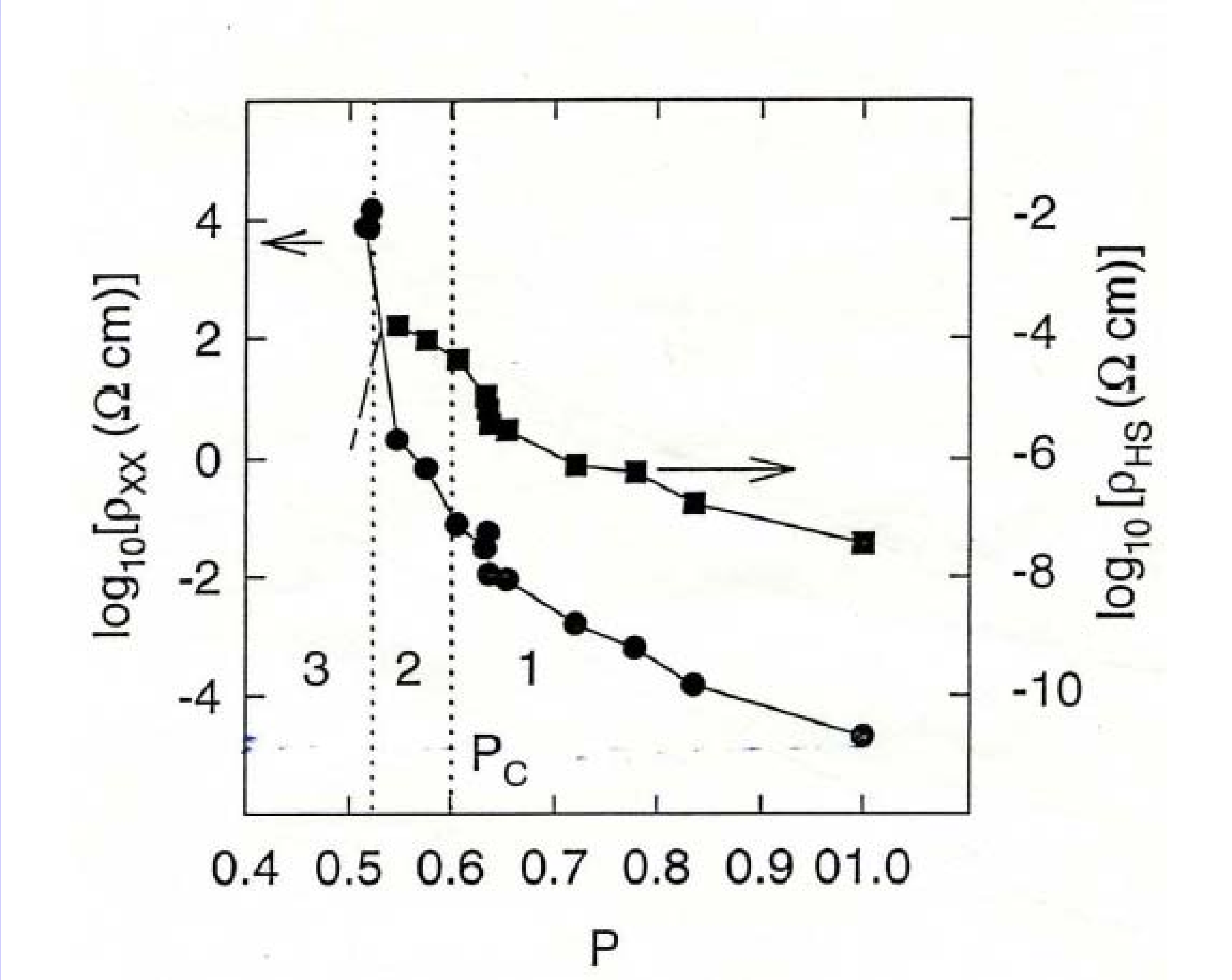

A. Pakhomov 1994

Conclusion 1-bad news

If magnetization in the sample is due to ferromagnetic or superparamagnetic clusters the sample exhibits AHE and AHE resistivity is linear to magnetization.

Observation of AHE can not be considered as a strict evidence of intrinsic ferromagnetism in diluted magnetic semiconductors

Co-occurrence of Superparamagnetism and Anomalous Hall Effect in Highly Reduced Cobalt Doped Rutile $TiO_{2-\delta}$ Films

S. R. Shinde[1,*], S. B. Ogale[1,2], J. S. Higgins[1], H. Zheng[2], A. J. Millis[3], V.N. Kulkarni[1,+], R. Ramesh[1,2], R. L. Greene[1], and T. Venkatesan[1]

[1]Center for Superconductivity Research, Department of Physics, University of Maryland, College Park, MD 20742-4111
[2]Department of Materials and Nuclear Engineering, University of Maryland, College Park, MD 20742-42111
[3]Department of Physics, Columbia University, 538 West 120th Street, New York, New York 10027

We report a detailed magnetic and structural analysis of highly reduced Co doped rutile $TiO_{2-\delta}$ films displaying an anomalous Hall effect (AHE). The temperature and field dependence of magnetization, and transmission electron microscopy clearly establish the presence of nano-sized superparamagnetic cobalt clusters of ~8–10 nm size in the films at the interface. The co-occurence of superparamagnetism and AHE raises questions regarding the use of the AHE as a test of the intrinsic nature of ferromagnetism in diluted magnetic semiconductors.

There is no correlation between AHE and resistivity in heterogeneous alloys

Two basic models and 4 types of SOI

Itinerant Magnetism

$$H^U_{so} = \frac{\hbar}{2m^2c^2}\left[\vec{\nabla} U(\vec{r}) \times \vec{p}\right]\vec{s}$$

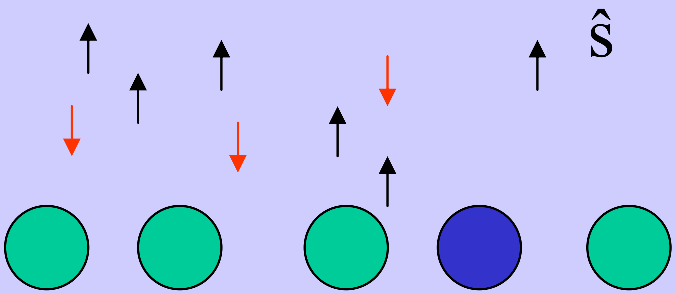

$$H^V_{so} = \frac{\hbar}{2m^2c^2}[\vec{\nabla} V(\vec{r}) \times \vec{p}]\vec{s}$$

Spin of current carrier (electron or hole) with its orbital moment

Localized Magnetism

$$(H^U_{so})^i_{sc} = \sum_{j\neq i} \frac{\hbar}{2m^2c^2}[\vec{\nabla} U_{ij} \times \vec{p}_j]\vec{s}_j$$

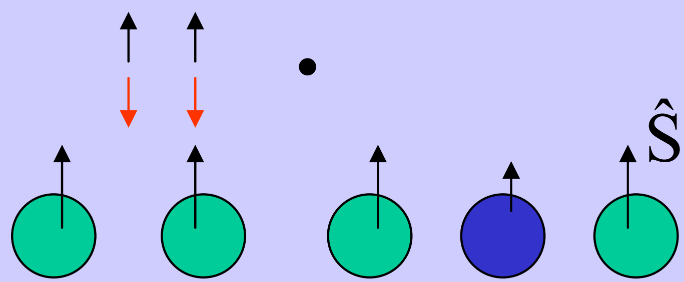

$$(H^V_{so})^i_{sc} = \sum_{j\neq i} \frac{\hbar}{2m^2c^2}[\vec{\nabla} V_{ij} \times \vec{p}_j]\vec{S}_j.$$

Orbital moment of current carrier with localized spin

Conclusion 2 – bad news

AHE may exist even if there is no spin polarization of charge current carriers

Observation of AHE in diluted magnetic semiconductors and oxides is not strict evidence of spin polarization of charge carriers

$$R_s = \frac{\sigma_{xy}(M_z)}{4\pi M_z(\sigma_{xx}+\sigma_{xy})^2} \approx \frac{\sigma_{xy}(M_z)}{4\pi M_z}\rho^2,$$

$$R_o = \frac{\sigma_{xy}(B_z)}{B_z(\sigma_{xx}+\sigma_{xy})^2} \approx \frac{\sigma_{xy}(B_z)}{B_z}\rho^2,$$

$$\frac{\Delta\rho}{\rho}(H_z) = \frac{\rho(H_z)-\rho(0)}{\rho(0)} = \beta\frac{M_z^{\,2}}{M_s^{\,2}}$$

$$\frac{\sigma_{xy}(M_z)}{4\pi M_z} = A(1+\alpha\frac{M_z^{\,2}}{M_s^{\,2}}),$$

$$\frac{\sigma_{xy}(B_z)}{B_z} = C(1+\gamma\frac{M_z^{\,2}}{M_s^{\,2}}),$$

$$R_s = R_s(0)\left[1+\alpha\frac{M_z^{\,2}}{M_s^{\,2}}\right]\left[1+\beta\frac{M_z^{\,2}}{M_s^{\,2}}\right]^2$$

$$R_0 = R_0(0)\left[1+\gamma\frac{M_z^{\,2}}{M_s^{\,2}}\right]\left[1+\beta\frac{M_z^{\,2}}{M_s^{\,2}}\right]^2$$

Conclusion 3 – be carefull

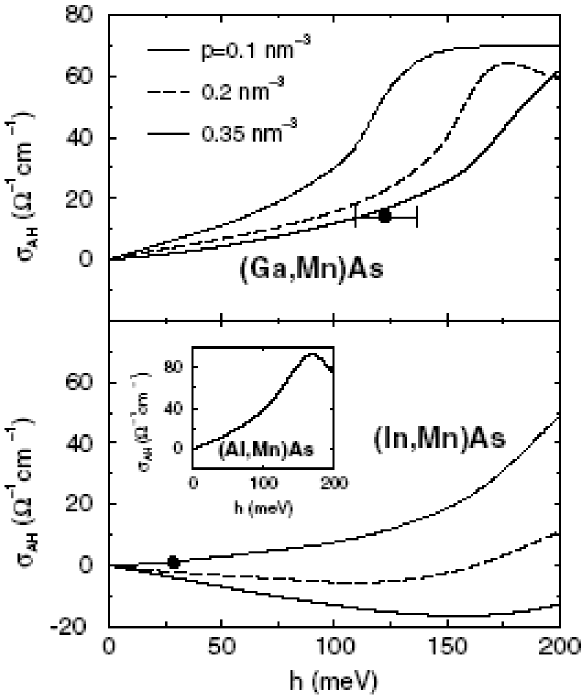

FIG. 2. Full numerical simulations of σ_{AH} for GaAs host (top panel), InAs host (bottom panel), and AlAs host (inset) with hole densities $p = 0.1$ nm^{-1} (dotted lines), $p = 0.2$ nm^{-1} (dashed lines), and $p = 0.35$ nm^{-1} (solid lines). Luttinger parameters of the valence bands were obtained from Ref. [32]. Filled circles in the top and bottom panels represent measured AHE [1,3,9]. The saturation mean-field h values for the two points were estimated from nominal sample parameters [1,3,9]. Horizontal error bars correspond to the experimental uncertainty of the J_{pd} coupling constant. Experimental hole density in the (Ga,Mn)As sample is $p = 0.35$ nm^{-1}; for (In,Mn)As, $p = 0.1$ nm^{-1} was determined indirectly from sample's transition temperature.

VOLUME 88, NUMBER 20 PHYSICAL REVIEW LETTERS 20 MAY 2002

Anomalous Hall Effect in Ferromagnetic Semiconductors

T. Jungwirth,[1,2] Qian Niu,[1] and A. H. MacDonald[1]
[1]*Department of Physics, The University of Texas, Austin, Texas 78712*
[2]*Institute of Physics ASCR, Cukrovarnická 10, 162 53 Praha 6, Czech Republic*
(Received 3 October 2001; published 6 May 2002)

We present a theory of the anomalous Hall effect in ferromagnetic (III, Mn)V semiconductors. Our theory relates the anomalous Hall conductance of a homogeneous ferromagnet to the Berry phase acquired by a quasiparticle wave function upon traversing closed paths on the spin-split Fermi surface. The quantitative agreement between our theory and experimental data in both (In, Mn)As and (Ga, Mn)As systems suggests that this disorder independent contribution to the anomalous Hall conductivity dominates in diluted magnetic semiconductors. The success of this model for (III, Mn)V materials is unprecedented in the longstanding effort to understand origins of the anomalous Hall effect in itinerant ferromagnets.

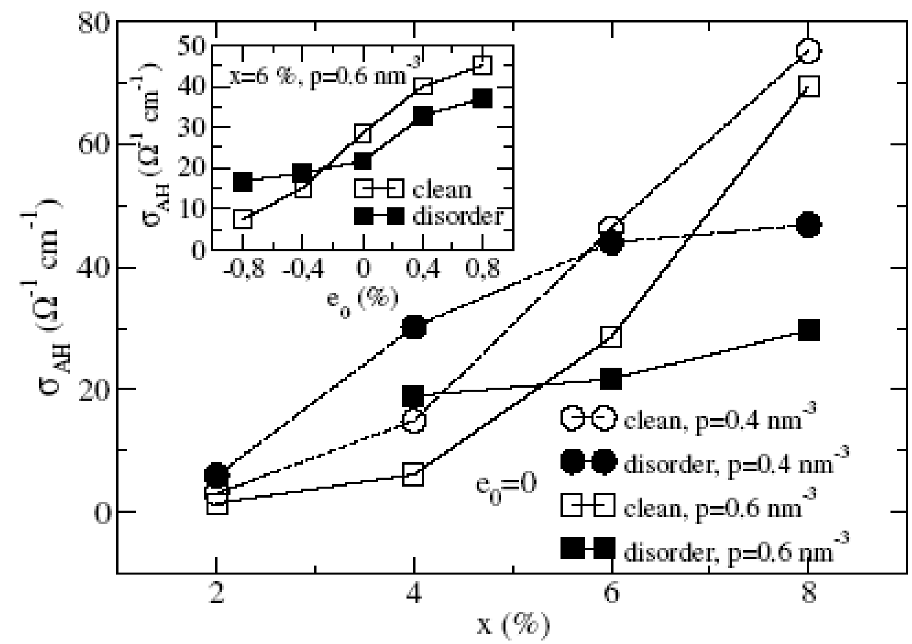

Fig. 4. Theoretical anomalous Hall conductivity of $Mn_xGa_{1-x}As$ DMS calculated in the clean limit (open symbols) and accounting for the random distribution of Mn and As-antisite impurities (filled symbols). (After Ref. 52.)

APPLIED PHYSICS LETTERS 91, 012502 (2007)

Anomalous Hall effect in anatase Co:TiO$_2$ ferromagnetic semiconductor

R. Ramaneti, J. C. Lodder, and R. Jansen[a)]

ysics, MSU

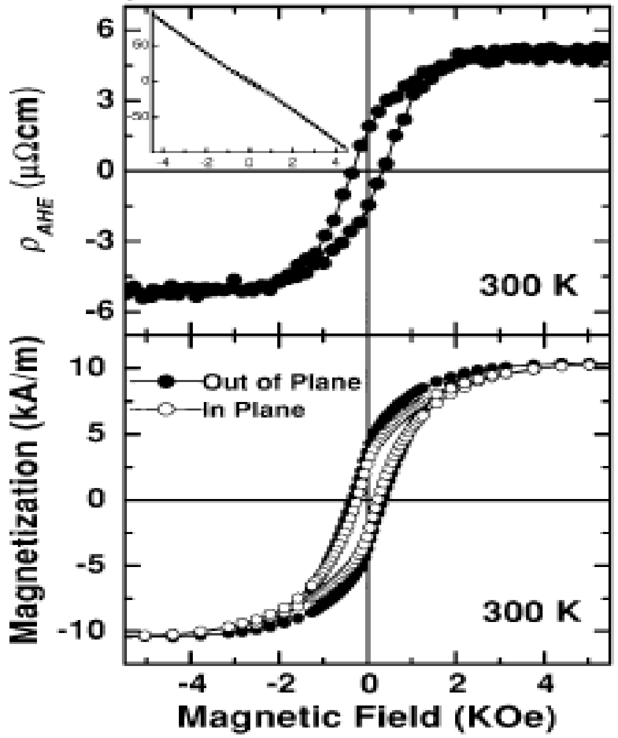

FIG. 1. Top panel: Anomalous Hall resistivity vs the out-of-plane applied magnetic field for a 550 nm Co:TiO$_2$ thin film. The data are obtained from the total Hall resistivity shown in the inset by subtracting the linear term due to the OHE. The inset has the same units as the main panel. Bottom panel: Magnetization with the field applied in plane (open circles) and out of plane (solid circles) of the same sample. All measurements were done at room temperature.

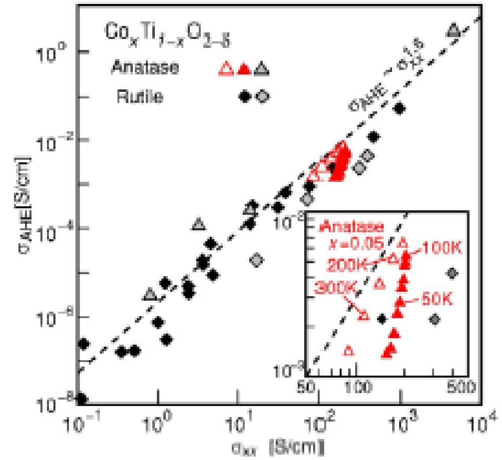

FIG. 20 Plot of AHE conductivity σ_{AHE} vs. conductivity σ for anatase Ti$_{1-x}$Co$_x$O$_{2-\delta}$ (triangles) and rutile Ti$_{1-x}$Co$_x$O$_{2-\delta}$ (diamonds). Grey symbols are data taken by other groups. The inset shows the expanded view of data for anatase with $x = 0.05$ (the open and closed triangles are for $T > 150$ K and $T < 100$ K, respectively. [From Ref. Ueno *et al.*, 2007.]

In thin-film samples of the ferromagnetic semiconductor anatase Ti$_{1-x}$Co$_x$O$_{2-\delta}$, Ueno *et al.* (Ueno *et al.*, 2008) have reported scaling between the AHE resistance and the magnetization M. The AHE conductivity σ_{xy}^{AH} scales with the conductivity σ_{xx} as $\sigma_{xy}^{AH} \propto \sigma_{xx}^{1.6}$ (Fig. 20). A similar scaling relation was observed in another polymorph rutile. See also Ref. Ramaneti *et al.*, 2007 for related work on Co-doped TiO$_2$.

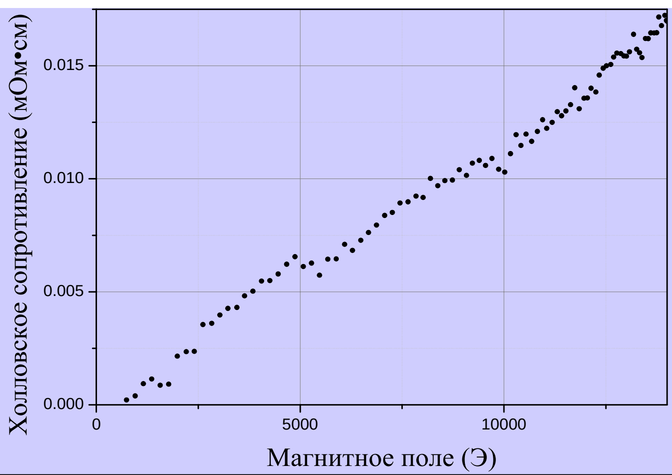

←

Yu. Mikhailovsky

Magnetism in Semiconducting Oxides, 2007: 69-86 ISBN: 81-7895-264-5
Editor: Nguyen Hoa Hong

4 Anomalous Hall effect in magnetic semiconductors

Jinke Tang
Department of Physics, University of New Orleans, New Orleans, LA 70148
USA

THANK YOU !